iScience

CellPress
OPEN ACCESS

Article

NADPH performs mediated electron transfer in cyanobacterial-driven bio-photoelectrochemical cells

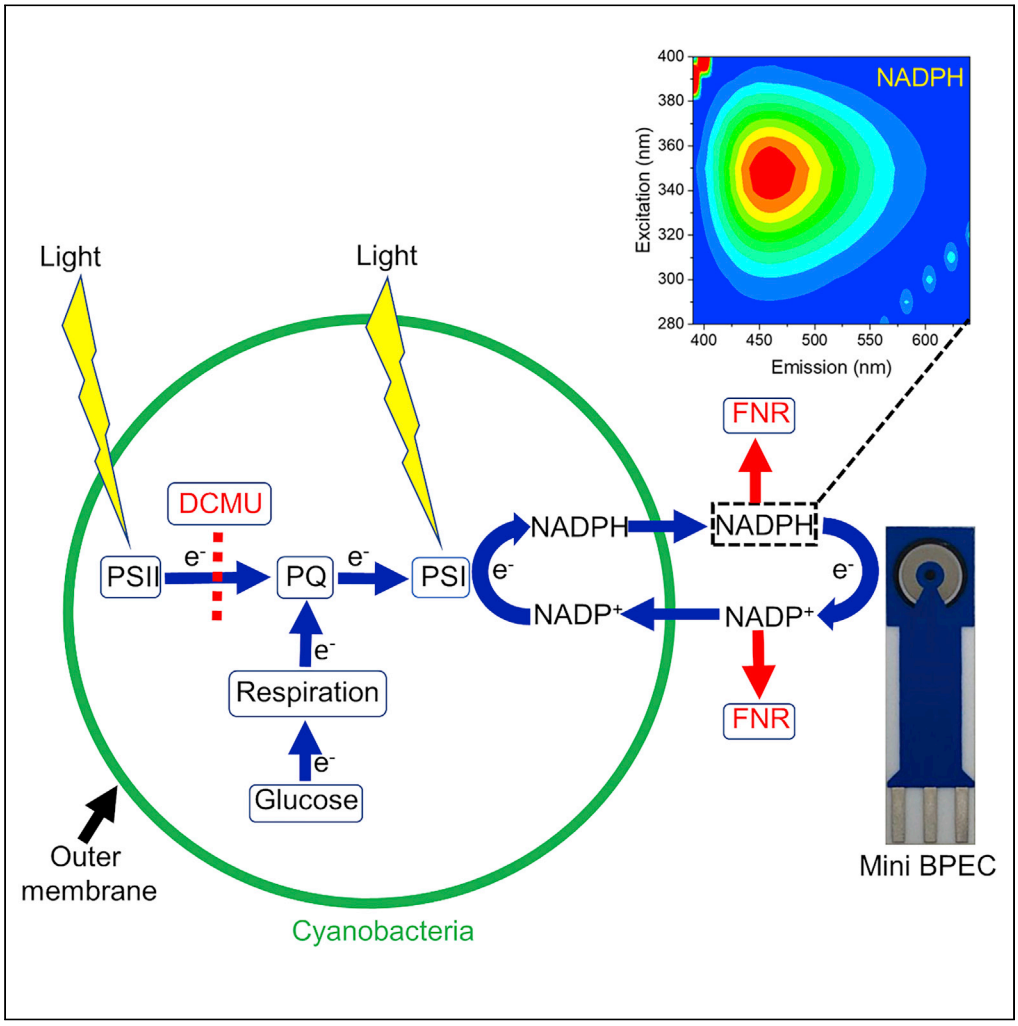

Yaniv Shlosberg, Benjamin Eichenbaum, Tünde N. Tóth, Guy Levin, Varda Liveanu, Gadi Schuster, Noam Adir

gadis@technion.ac.il (G.S.)
noam@ch.technion.ac.il (N.A.)

HIGHLIGHTS

NADPH is the electron mediator in cyanobacterial bio-photoelectrochemical cells

Operation of the electrochemical cell induces NADPH release from cyanobacteria

Addition of exogenous $NADP^+$ to cyanobacteria enhances photocurrent production

NADPH is released by different fresh or sea water cyanobacterial species

Shlosberg et al., iScience *24*, 101892
January 22, 2021
https://doi.org/10.1016/j.isci.2020.101892

iScience

CellPress
OPEN ACCESS

Article

NADPH performs mediated electron transfer in cyanobacterial-driven bio-photoelectrochemical cells

Yaniv Shlosberg,[1,2] Benjamin Eichenbaum,[3] Tünde N. Tóth,[1,2] Guy Levin,[3] Varda Liveanu,[3] Gadi Schuster,[1,3,*] and Noam Adir[1,2,4,*]

SUMMARY

Previous studies have shown that live cyanobacteria can produce photocurrent in bio-photoelectrochemical cells (BPECs) that can be exploited for clean renewable energy production. Electron transfer from cyanobacteria to the electrochemical cell was proposed to be facilitated by small molecule(s) mediator(s) whose identity (or identities) remain unknown. Here, we elucidate the mechanism of electron transfer in the BPEC by identifying the major electron mediator as NADPH in three cyanobacterial species. We show that an increase in the concentration of NADPH secreted into the external cell medium (ECM) is obtained by both illumination and activation of the BPEC. Elimination of NADPH in the ECM abrogates the photocurrent while addition of exogenous $NADP^+$ significantly increases and prolongs the photocurrent production. $NADP^+$ is thus the first non-toxic, water soluble electron mediator that can functionally link photosynthetic cells to an energy conversion system and may serve to improve the performance of future BPECs.

INTRODUCTION

World energy consumption continues to increase each year. To meet the increasing demand, use of fossil fuels continues at ever growing amounts, and as a result, more pollution is released into the environment. Estimation of the energy consumption between the years 2008 and 2035 has predicted an increase of >50 % that will reach an annual average of ~26 TW (U.S. IEA, 2011). The increase in pollution has recently become a major concern because it might cause severe climate change which will be globally detrimental. Therefore, there is an urgent need for replacement of polluting energy production technologies with non-polluting, renewable, green energy technologies.

One such technology, which is believed to be a good base for production of green energy, is microbial fuel cells (MFCs). The main principle of MFCs is to use bacteria in electrochemical cells as electron donors (Fang et al., 2020; Park et al., 1999) at the anode or acceptors (Bergel et al., 2005; Fang et al., 2020; Gregory et al., 2004) at the cathode. The electron transfer between the inner membrane of live bacteria and the anode of the electrochemical cell was first demonstrated by Potter in 1910 (Ieropoulos et al., 2005). Since the membranes of most bacterial species have low conductivity, MFCs utilize small molecules which can mediate electrons between the inner membrane and the electrodes. Over the years, the use of various bacterial species has been reported (Bond et al., 2002; Bond and Lovley, 2003; Chaudhuri and Lovley, 2003; Choi et al., 2003; Gregory et al., 2004; Kim et al., 1999; Lee et al., 2002; Liu et al., 2006; Menicucci et al., 2006; Min et al., 2005; Park and Zeikus, 2002; 2000; 1999; Park et al., 1999; Pham et al., 2003; Rabaey et al., 2005; 2004; Rhoads et al., 2005; Ringeisen et al., 2006; Tanaka et al., 1983; Thurston et al., 1985; U.S. IEA, 2011; Wei et al., 2016). Some of these species were able to produce endogenous electron mediators (Bond et al., 2002; Bond and Lovley, 2003; Chaudhuri and Lovley, 2003; Liu et al., 2006; Min et al., 2005; Pham et al., 2003). Addition of different exogenous electron mediators was reported to significantly increase the produced current including cystine, neutral red, thionin, sulphides, ferric chelated complexes, quinones, phenazines, and humic acids (Ieropoulos et al., 2005; Lovley et al, 1996, 2004; Rabaey et al, 2004, 2005; Simoska et al., 2019). As most of these compounds are considered to be toxic, their use must be tightly regulated. Current production can also be performed by direct electron transfer (DET) mechanisms. Such a mechanism was reported for *Geobacter sulfurreducens* biofilms which use conductive pili and *c*-type cytochromes

[1]Grand Technion Energy Program, Technion, Haifa 32000, Israel

[2]Schulich Faculty of Chemistry, Technion, Haifa 32000, Israel

[3]Faculty of Biology, Technion, Haifa 32000, Israel

[4]Lead Contact

*Correspondence: gadis@technion.ac.il (G.S.), noam@ch.technion.ac.il (N.A.)

https://doi.org/10.1016/j.isci.2020.101892

to reduce the anode (Heidary et al., 2020; Lovley, 2012; Nevin et al., 2008; Yi et al., 2009). *Shewanella oneidensis* MR-1 biofilms were reported to conduct direct electron transfer through Mtr complexes (Hartshorne et al., 2007; Shi et al., 2012) and an indirect electron transfer which is mediated by flavin molecules.

Recent studies have shown that oxygenic and anoxygenic photosynthetic microorganisms can be used as the source of electrons that can be collected in bio-photoelectrochemical cells (BPEC) for solar energy conversion to electrical current and/or clean fuels (such as hydrogen) (Grattieri, 2020; Grattieri et al., 2019a, 2019b; Tschörtner et al., 2019). Therefore, it has been suggested that their use could serve as the main photo-active component in the development of innovative renewable energy applications (Deng and Coleman, 1999; Efrati et al., 2016; Gizzie et al., 2015; Grattieri, 2020; Kaiser et al., 2013; Larom et al., 2015; McCormick et al, 2011, 2015; Pinhassi et al., 2016; Sawa et al., 2017; Schmetterer et al., 1994; Sekar et al, 2014, 2016; Zhang et al., 2013; Zhao et al., 2015). In some systems, light energy was converted utilizing reaction center/light harvesting proteins (Mershin et al., 2012) or isolated photosystems conductively attached to electrodes in BPECs (Bombelli et al., 2015; Efrati et al, 2013, Efrati et al., 2016; Hartmann et al., 2020; Li et al., 2016; Yehezkeli et al., 2012; Zhao et al., 2014). Some of these systems require the addition of an exogenous mediator and the photosystems must be attached to the anode which can be done by utilizing an immobilized electron mediator such as redox polymer (Zhao et al., 2014). Use of Photosystem I (PSI) or reaction centers from non-oxygenic photosynthetic organisms requires addition of an electron donor (Efrati et al, 2013, Efrati et al., 2016; Hartmann et al., 2020; Zhao et al., 2015), while in systems based on Photosystem II (PSII), water serves as the initial electron donor (Bombelli et al., 2015). Use of isolated complexes, especially when PSII is utilized, is hampered by their relative instability, leading to loss of activity. Utilization of thylakoid membranes, whose isolation process is much easier and cheaper than isolating complexes (Hasan et al., 2017; Pinhassi et al., 2016), entails only cell disruption and centrifugation, without expensive detergent treatment and chromatography. While the complexes are still unstable and cannot be repaired, replacement with fresh aliquots of membranes is inexpensive and non-polluting. However, their ability to perform DET is significantly lower than that of the isolated complexes, leading to use of mediating molecules. A potentially more stable system can be achieved by utilizing living photosynthetic microorganisms, which have internal repair mechanisms for replacing photodamaged components. Use of intact cells in BPECs leads to a new problem however: how to enable external electrodes to acquire electrons from internal membrane components that are sequestered behind multiple layers of membranes that make up the external barrier of the cells.

This problem can be solved by performing mediated electron transfer (MET) with mediators that are able to cross these barriers and efficiently interact with either inorganic or metallic electrodes and photosynthetic biological components. Previous studies have used exogenously added mediators such as ferricyanide (Huang et al., 2015; Lan et al., 2013; Laohavisit et al., 2015; McCormick, 2011, 2013; Ochiai et al., 1983), 2,6-dichloro-1,4 benzoquinone (Calkins et al., 2013; Larom et al., 2010; Pinhassi et al, 2015, 2016; Sekar et al., 2014; Tanaka et al., 1985), 2-hydroxy-1,4-naphthoquinone (Tanaka et al., 1988; Torimura et al., 2001; Yagishita et al., 1993; Zou et al, 2009, 2010), or 1,4-benzoquinone (Longatte et al., 2018; Sekar et al., 2014). However, all bacteria, and especially cyanobacteria, have outer membranes that limit the ability of such molecules to enter and exit the cells. Some of the mediators are toxic and most have a low solubility in water-based media (Cereda, 2014). The use of exogenous mediators might be avoided using a semi-dry cyanobacterial monolayer which can produce current by a DET mechanism (Sekar et al., 2016; Thirumurthy et al., 2020; Wei et al., 2016); however, such systems might damage the survival of the cyanobacteria and limit its ability to multiply which might be very important for construction of useful systems. One of the possible mechanisms for DET with cyanobacteria is through type IV pili. However, in a recent study, no significant difference was found between the photocurrent production of *wt Synechocystis* and the pili-deficient mutant ΔpilD (Thirumurthy et al., 2020). A different option for cyanobacteria is MET that could be conducted by an endogenous mediator which can be secreted by the cells in similar with other small inorganic molecules that can pass the outer membrane through porin channels (Kowata et al., 2017). It has recently been shown that live cyanobacteria can also produce photocurrent without the addition of any exogenous mediator (Saper et al., 2018). It was suggested that the electron source originates from contributions of both the photosynthetic and respiratory pathways which can combine use reduced plastoquinone molecules which then continue to transfer electrons between a sequence of molecules until they reach the final step of the photosynthetic pathway, which is the reduction of $NADP^+$ to NADPH (Saper et al., 2018). It was proposed that these reducing equivalents could then reduce metabolites that can be either passively or actively transported out of the cells and serve to mediate the biological

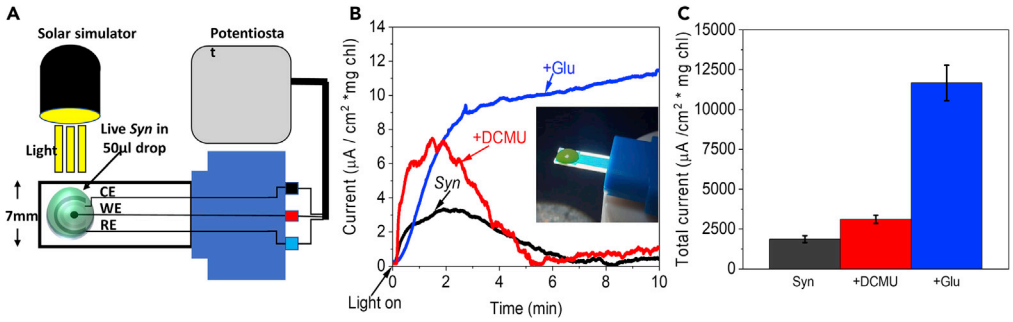

Figure 1. Light-dependent generation of electricity by live *Syn*

Syn cells (5µg chlorophyll) were placed in a 50-µL drop on a minielectrode-based BPEC, and the light-dependent chronoamperometry (CA) measurement was performed applying a voltage bias of 0.5 V on the anode.

(A) Schematic drawing of the mini-BPEC setup.

(B) CA of the light-dependent produced current of live *Syn* (black), with the addition of 100 µM of the herbicide DCMU (+DCMU, red) and after a pre-incubation in dark for 1 hr with 5 mM glucose (+Glu, blue). A picture of the minielectrode BPEC is shown in the inset.

(C) Calculation of the total current that was accumulated during 10 min in CA measurements of *Syn* (black), +DCMU (red), and +glucose (blue). The error bars represent the standard deviation over 3 independent measurements.

processes with an electrochemical cell. Efforts were made to identify the endogenous mediators using cyclic voltammetry and metabolomic measurements of the cyanobacterial external cell medium (ECM). However, the identity of the mediator(s) remained elusive (Saper et al., 2018).

In the present work, we use two-dimensional fluorescence map (2D-FM) fingerprinting to identify NADPH as a major component that is exported from cyanobacteria and accumulates in the BPEC medium upon the application of light and electric potential. NADH can also mediate between the cells and the BPEC, but it is not accumulated in the external medium upon illumination. Therefore, NADPH serves as the endogenous electron mediator of cyanobacteria, and since its addition to the system increased the produced electrical current, this finding would assist the generation of bio-photoelectrochemical devices that use living photosynthetic organisms to produce electricity and hydrogen.

RESULTS AND DISCUSSION

Light-dependent generation of electricity by live *Synechocystis* in a mini-BPEC system

We have previously shown that photocurrent could be produced by live *Synechocystis sp. PCC 6803* (*Syn*) cells in a BPEC (Saper et al., 2018). This BPEC was composed of 3 bulk electrodes: a graphite disk anode (the working electrode [WE]), a platinum rod cathode (the counter electrode [CE]), and an Ag/AgCl/3M NaCl reference electrode (RE), with direct contact between the cells and the anode in 50 mL of buffered solution. The large ECM volume made chemical identification of the internal mediator, released from the cyanobacteria, difficult (Saper et al., 2018). In order to chemically analyze the BPEC solution and identify the mediator, while measuring current, we utilized commercial screen-printed electrode (SPE) systems that formed the basis of a mini-BPEC, where a minimal ECM volume would be sufficient. The new mini-BPEC consisted of SPEs with carbon WE anode (0.79 mm^2), platinum CE cathode, and Ag coated with AgCl RE enabling recording a current of about 3 µA cm^{-2} using 50 µL live *Syn* cells (containing 5 µg of chlorophyll, about $1.4x10^8$ cells) (Figure 1A). In agreement with the previous results that were obtained with the larger BPEC (Saper et al., 2018), live *Syn* cells produced appreciable light-dependent electrical current without the addition of an exogenous electron mediator. In addition, as previously reported for the large BPEC, the current remained constant for a longer period of time when the cells were pre-incubated with glucose (Glu, Figures 1B and 1C) (Larom et al., 2015; Saper et al., 2018). Addition of Glu enhances the activity of the respiratory pathway, generating a multistep reduction process that ends in reduction of plastoquinone molecules (PQs). PQs are also an intermediate electron carrier in the photosynthetic pathway. Therefore, they link between the two pathways and continue to transfer electrons downstream in a multistep reduction process that ends in reduction of $NADP^+$ to NADPH. Addition of the herbicide 3-(3,4-dichlorophenyl)-1,1-dimethylurea (DCMU), which inhibits the electron flow from PSII downstream the photosynthetic pathway to the PQ, was shown to significantly enhance the photocurrent (Saper et al.,

2018). It was concluded that the electron source from the cyanobacteria is the respiratory pathway from which the electrons are transferred to PSI and from this light-driven reaction to an internal mediator(s) that is/are secreted from the cell and reduce(s) the graphite anode (Saper et al., 2018). In addition, it was reported that PSII is not the major source of electrons in this pathway since the enhancing effect of DCMU happens also with *Syn* mutant lacking PSII (Saper et al., 2018). The reason why addition of DCMU increases the photocurrent in cyanobacterial BPECs is still unclear. In our previous work, we suggested that DCMU affects the production of the photocurrent at secondary site(s) by either inhibiting forward electron flow within the respiratory system or by enhancing the release of the external electron mediator (Saper et al., 2018). It has been shown that unlike plants or green algae, DCMU effects additional cyanobacterial functions. Addition of DCMU has been shown to affect Mn^{2+} uptake and release (Keren et al., 2002), Fe^{3+} reduction (Kranzler et al., 2014), and increase in the flexibility of thylakoid membranes in light (Stingaciu et al., 2019). When the ECM was collected following operation of the mini-BPEC and filtered through a 3 kDa filter, the filtrate was able to reduce oxidized cytochrome *c* (Figure S1). When the *Syn* cells were not illuminated in the mini-BPEC, no current was obtained (Figure S2).

In our previous work using the 50 mL BPEC, we have found that mechanical treating the live *Syn* by a low-pressure microfluidizer or by osmotic shock significantly enhanced the amount of current produced in the BPEC (Saper et al., 2018). To simplify our system, in the following experiments, the cells were not pre-treated, other than centrifugation from their growth medium (see Transparent Methods for additional details). All other experimental parameters are similar to those previously described (Saper et al., 2018), and we assume that the same reactions occur on the CE, including reduction of protons to molecular hydrogen, as well as reduction of other molecules in the ECM.

Identification of NADPH and/or NADH in the ECM.

Production of photocurrent from live *Syn* without addition of an exogenous electron mediator has been suggested to occur by the secretion of endogenous electron mediator(s) to the ECM. We previously performed metabolomic assays on whole cells used in the BPEC (Saper et al., 2018); however, no significant change in any of the known metabolites could be observed. The stability of redox molecules in the ECM may be low. Therefore, we wished to utilize less destructive spectroscopic methods to screen the ECM for known redox components. Absorption spectra, FTIR, and NMR measurements did not result in the identification of a known redox-active molecule, especially due to the challenge of the presence of hundreds of molecules in the ECM mixture. Another method that can identify molecule(s) in the ECM is 2D-FMs, as many redox-active molecules contain moieties that absorb and fluoresce energy at specific wavelengths. When the ECMs, taken following the current production experiment in the BPEC, were analyzed by this method, a strong signal that matched the fluorescence fingerprint of NADPH and/or NADH (NAD(P)H) was observed. The signal in the ECM was compared to commercial samples of NAD(P)H used as standards and to previously published measurements of these molecules (Dartnell et al., 2010) (Figure 2). It should be noted that the 2D-FM analysis measures the sum of NADP(H) that is present in the solution at the moment of removal of the cells from the BPEC followed by cell removal by filtration. The total concentration of both of these species is of course greater than the immediate concentration of NADPH that is transferring electrons to the anode at any given moment, as only a subset of molecules are attractively associated with the anode.

Accumulation of NAD(P)H in the ECM is dependent on light and the connection between the cells and the electrochemical system

We suggest that the presence of NAD(P)H in the ECM is the result of the secretion of NADH, NADPH, or both to the ECM by the live *Syn*. Therefore, we next ask if this secretion is light dependent and whether or not it depends on physical linkage between the cells and the electrochemical system in the mini-BPEC. To this end, we performed 2D-FM spectra on the ECM from *Syn* cells, which were kept in the dark or exposed to light in either small transparent test tubes or in the mini-BPEC on the electrodes during 100 s of chronoamperometry (CA) measurement. No significant difference was observed between the fluorescence of the ECMs which were illuminated or not illuminated without any connection to the electrochemical system (in tubes). The NAD(P)H fluorescence intensity of *Syn* ECMs after CA measurement was significantly higher and further enhanced about upon illumination (Figure 3). NADPH is involved in a variety of enzymatic processes in the periplasmic space, and export of NADPH from the cyanobacterial cells to the ECM is prevented by the outer cell membrane. Under certain condition, cells invest energy to import NAD^+ (released from lysed cells in the culture) which is an important molecule in many biological processes (Gruber and Haferkamp, 2019; Major et al., 2017; Murakawa and Takahashi, 1978; Zhou et al., 2011).

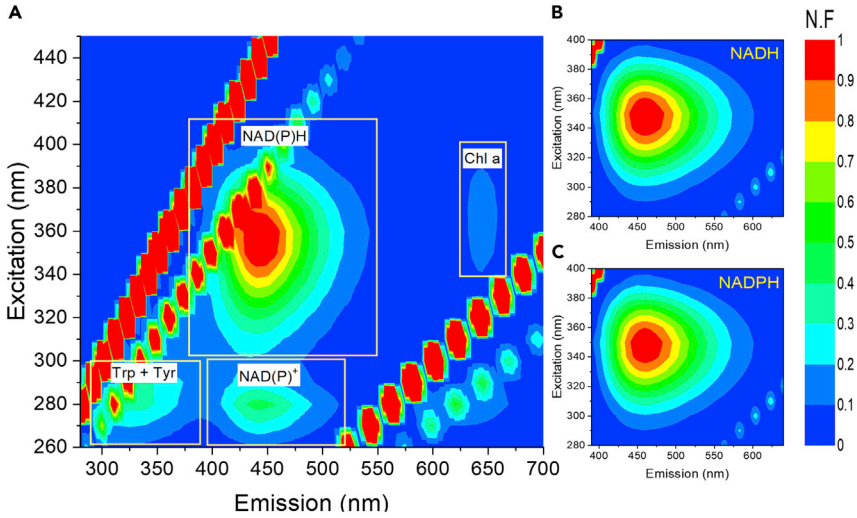

Figure 2. Identification of NAD(P)H in the ECM

Normalized 2D-FM spectra of the ECM of *Syn*, NADH, and NADPH.

(A) Normalized 2D-FMs of the ECM of *Syn* spectral fingerprints of the NAD(P)H, $NAD(P)^+$, the amino acids Trp and Tyr, and chl *a* are marked above each peak. The lines of diagonal spots that appear in all of the maps presented here and in the following figures result from light scattering of the xenon lamp and Raman scattering of the water (Lawaetz and Stedmon, 2009).

(B) Normalized 2D-FM spectra of 5 mM NADH.

(C) Normalized 2D-FM spectra of 5 mM NADPH. In all panels, normalization was done by division of the intensity values of the whole map by the value of NAD(P)H signal obtained at (λ(ex) = 350, λ(em) = 450 nm). The fluorescence intensities in the color bar are displayed as normalized fluorescence (N.F).

However, when the cells become a component in a bio-electrochemical cell, they export more NADPH. Activation of the BPEC changes the distribution of the ions (including protons) that are associated with the cyanobacterial cell wall, as well as on the surface of the anode. Such ionic changes on the cell surface may impact the permeability of the outer cell wall (Vaara, 1992). In order to determine the NAD(P)H concentration in the *Syn* ECM, a calibration curve of NADH concentration vs. fluorescence intensity was prepared based on NADH fluorescence (Figure S3). The calibration assumes that the 2D-FM of NADH and NADPH is spectrally identical under these conditions of measurement, as has been described by others (Blacker et al., 2014). While addition of DCMU to the *Syn* cells increases the current 2-fold (Figure S4), the change in the concentration of NADPH in the ECM was beyond the resolution of the 2D-FM method.

In order to estimate the ability of exogenous NADPH to produce photocurrent in the BPEC, 1μM NADPH was added with or without *Syn* cells (Figure S5A). In both measurements, a fast increase of about 4 μA was obtained followed by a fast decrease of the current to the same level as it was prior to the addition within a few seconds. To evaluate the kinetics of the decay in measured current, we performed fitting analysis to the curve decay. The analysis showed that the mathematical decay function is exponential (Figure S5B). The fast current decay suggests that in order to maintain the current formation, cyanobacteria needs to continuously secrete NADPH to the ECM, whereas the active portion of NADPH that reaches the anode to reduce it is about 1 μM/sec at the maximal current values.

NAD(P)H concentrations were calculated for ECM of *Syn* solutions which were illuminated or not – illuminated in test tubes or on electrodes during CA measurements as shown in the insert in Figure 3B. As can be seen, illumination in the BPEC results with the accumulation of about ~2 μM NAD(P)H in the ECM. This concentration is about ten times greater than the amount of NAD(P)H that accumulates without any connection to the electrochemical system and about four times greater than accumulated without illumination. These results showed that the connection between the active electrochemical system and live *Syn* cells enhances secretion and accumulation of NAD(P)H in the ECM that can reduce the anode and produce electric current. Under illumination, the concentration of NAD(P)H in the cells is increased further; there is a concomitant increase in NAD(P)H release to the ECM and more current is produced. In the absence of connection to the electrochemical system, the release of NAD(P)H is low, and no significant difference can be observed

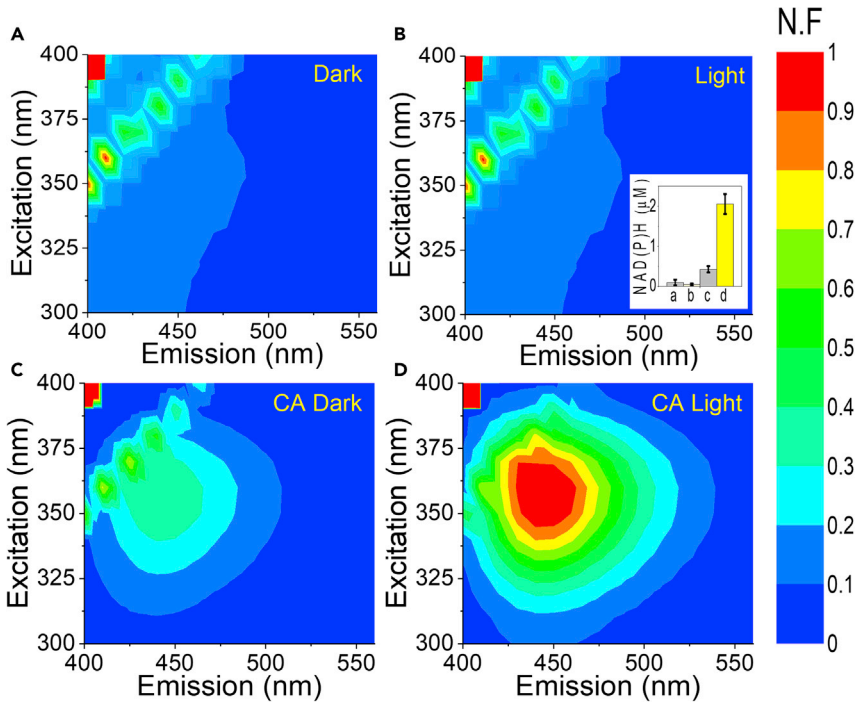

Figure 3. Accumulation of NAD(P)H in the ECM is dependent on light and the connection between the cells and the electrochemical system

2D-FM spectra of the ECM of *Syn* after incubation in test tubes or during CA measurements on the electrodes in dark or under illumination.

(A) In test tubes in the dark.

(B) In test tubes under illumination.

(C) On the electrodes after 100 s of CA measurement in the dark.

(D) On the electrodes after 100 s of CA measurement under illumination. The inset in (B) displays NAD(P)H concentrations which were calculated based on the fluorescence intensities at (λ(ex) 350 = nm, λ(em) = 450 nm). The error bars in the insert of (B) represents the standard deviation over 6 independent measurements. The fluorescence intensities in the color bar are displayed as normalized fluorescence (N.F).

between cells which were illuminated or not illuminated. These results show that in the absence of the electrochemical system, NAD(P)H release is not favored by the cells.

Under illumination, NADPH accumulates in the *Syn* ECM more than NADH

Enzymatic kits were used for quantification and differentiation between NADH and NADPH in the *Syn* ECM (see Transparent Methods for details). Both enzymatic assays were applied to the ECM of *Syn* after 100 s of CA measurements in either dark or under illumination. The presence of both NADH and NADPH was detected. No significant difference was found between NADH concentrations in the ECM of cells which were illuminated or not illuminated and was found to be about 0.6 μM (Figure 4). However, the concentration of NADPH in the ECM, following illumination, was higher, increasing from about 0.4 to 1.6 μM (Figure 4). The sum of NADH + NADPH concentrations is about 2 μM which is in agreement with the NAD(P)H concentration which was calculated based on the 2D-FMs. This result indicates that NADPH, rather than NADH, accumulates in the ECM in the light and suggests that this molecule may serve as the primary mediator of the light-dependent current. In contrast with NADPH formation by photosynthesis which increases during illumination, the concentration of NADH is not changed during illumination and any NADH found in the ECM is probably not due to the formation of new NADH molecules by a light-related process.

Addition of ferredoxin $NADP^+$ reductase eliminates both the light-dependent electric current and the NAD(P)H accumulation in the ECM

Ferredoxin $NADP^+$ reductase (FNR) binds both $NAD(P)^+$ and NAD(P)H (Batie and Kamin, 1986). In order to further support our identification of NAD(P)H as the main endogenous electron mediator, increasing

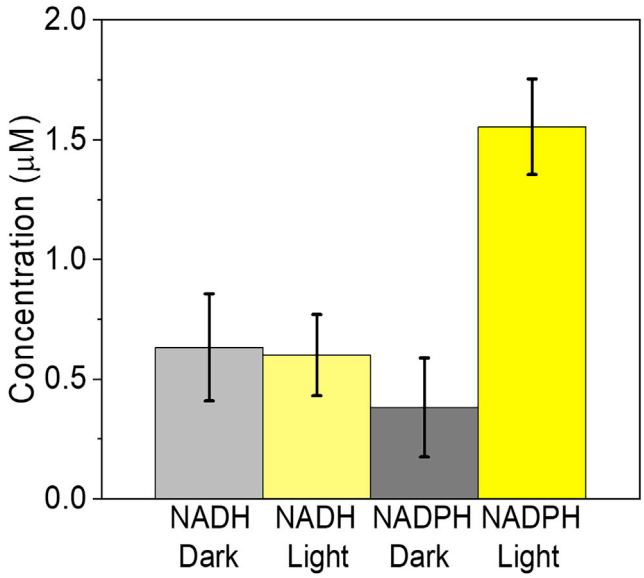

Figure 4. When illuminated, NADPH accumulates in the *Syn* ECM more than NADH

Quantification of NADH and NADPH concentrations in the ECM of *Syn,* after 100 s of CA measurement with or without illumination, was done using a chemical enzymatic assay. The error bars represent the standard deviation over 9 independent measurements.

concentrations of the enzyme FNR were added to *Syn* cells and CA was measured. We observed that the current was reduced as function of the increasing FNR concentrations and was almost totally abrogated at FNR concentration of 30 μM.

In order to make sure that the current was abrogated because of the specific binding activity of FNR and not by generic protein binding or changes in the conductance and rigidity of the electrolyte, the CA of *Syn* was measured with 1 mg/mL of bovine serum albumin (BSA). Addition of BSA did not significantly affect the photocurrent (Figure 5A). In addition, the experiment was repeated with 15 μM of a recombinant FNR enzyme whose origin is the green algae *C. reinardtii*. Addition of the CrFNR also abrogated the photocurrent (Figure S6).

In order to assess further whether the reduction in current was caused by FNR binding of NADPH and preventing it from being the mediator, *Syn* cells were incubated for 30 min with or without 1 mg/mL FNR which is a ~10-fold molar excess to that of the calculated NADP(H) concentration. The samples were then centrifuged in ultrafiltration devices with a 3kD filter. 2D-FMs (λ(ex) = 260–400 nm, λ(em) = 400–520 nm) of the filtrates were measured. The spectral fingerprint NAD(P)H was observed only in the filtrates of samples which did not contain FNR, indicating that NAD(P)H molecules were bound to FNR and therefore did not appear in the filtrate (Figures 5C and 5D). Since the addition of FNR almost completely abolished both photocurrent and the 2D-FM signal of NAD(P)H, these results imply that NADPH is the primary mediator of the electrons from *Syn* PSI to the graphite anode when generating the light-dependent electric current in the BPEC. As an additional control, we performed CA in the presence of exogenous NADPH added in excess of the concentration of the added FNR, and as expected, the current was not abrogated (Figure S7). Addition of DCMU, shown to increase the measured current from *Syn* cells, does not prevent the abrogation of the photocurrent by FNR (Figure S8)

Addition of an exogenous $NADP^+$ to the ECM enhances photocurrent production

There are two scenarios whereby NADPH can serve as the mediator in MET-type current production. In the first, NADPH is secreted but following electron transfer is not uptaken by the cells for additional cycles. In the second scenario, following oxidation, $NADP^+$ is uptaken for further cycles. To differentiate between these two scenarios, we performed a pre-incubation of *Syn* with exogenously added $NADP^+$ to observe whether indeed more NADPH would be produced under illumination resulting in an elevated electric

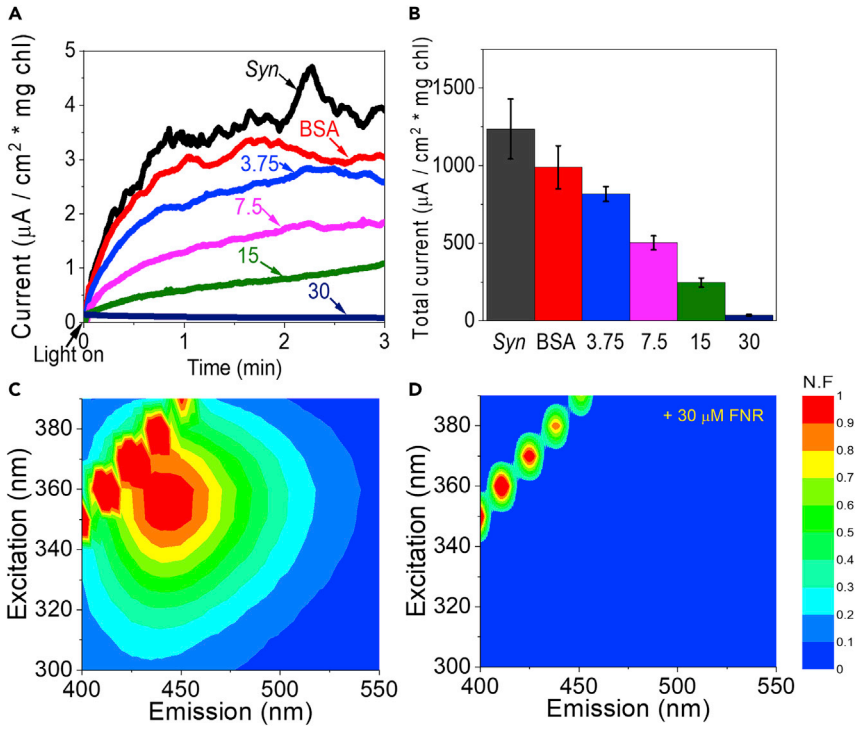

Figure 5. Addition of FNR that binds NAD(P)H eliminates both the light-dependent electric current and the NAD(P)H accumulation in the ECM

(A) CA of *Syn* (black) and *Syn* + BSA (red, negative control), and *Syn* + 3.75, 7.5, 15, and 30 μM FNR (light blue, magenta, green, and dark blue, respectively).

(B) Calculations of the current sum that was accumulated during 3 min in CA measurements of *Syn* (black), + *Syn* + BSA (red), and *Syn* + 3.75, 7.5, 15 and 30 μM FNR (light blue, magenta, green, and dark blue, respectively). The error bars represent the standard deviation over 3 independent measurements.

(C) 2D-FM of *Syn* filtrate.

(D) 2D-FM of *Syn* + FNR filtrate. The ECMs of *Syn*, with and without the addition of FNR at the concentration of 1 mg/mL, were filtrated through a 3 kD filter and measured with 2D-FMs. The fluorescence intensities in the color bar are displayed as normalized fluorescence (N.F).

current. We measured the BPEC photocurrent with 5 mM $NADP^+$ in the absence of cells or in the presence of *Syn* at different pre-incubation times (0–2 hr). In the absence of cells, addition of $NADP^+$ did not produce any significant photocurrent. In the presence of *Syn* cells, addition of $NADP^+$ significantly increased the photocurrent. The longevity, maximum, and total current all increased in correlation with the pre-incubation time (Figure 6A).

This result implies a mechanism whereby $NADP^+$ can enter and exit the cells and mediate electrons from the photosynthetic system (PSI) and the BPEC anode. Therefore, the addition of $NADP^+$ at a concentration higher than what is released from the cells can significantly increase the photocurrent. Although *Syn* does not produce current in dark, the possibility that addition of exogenous $NADP^+$ can produce dark current by mediating electrons was examined (Figure S9). CA of *Syn*, pre-incubated for 2 hr with 5mM $NADP^+$, was measured in dark and light. While current was obtained in the light, no photocurrent was produced in the dark. We postulate that in the absence of light, the uptake of exogenous $NADP^+$ into the cytoplasm may be inhibited or that lack of photosynthetic activity prevents $NADP^+$ reduction. Addition of exogenous $NADP^+$ in the light also significantly increased the current when measured with *Syn* cells in the large 50 mL BPEC previously described (Figure S10) (Saper et al., 2018).

Two additional cyanobacterial species export NAD(P)H and generate photocurrent

Our previous studies which showed that photocurrent can be produced without addition of an external electron mediator were focused on *Syn*. We wished to screen additional species in our mini-BPEC to assess

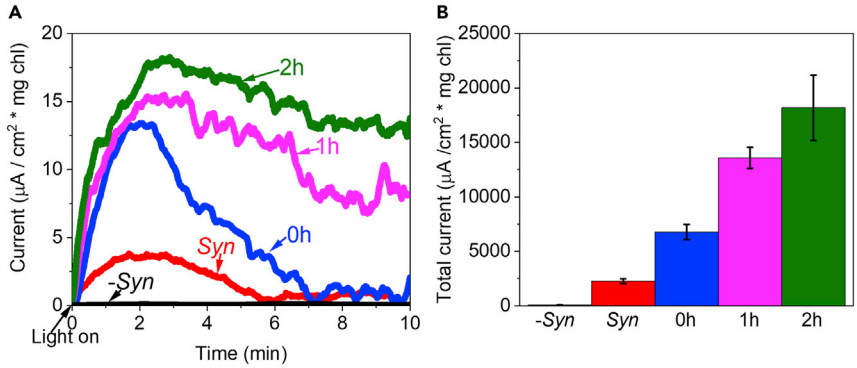

Figure 6. Addition of NADP$^+$ enhances photocurrent production

(A) CA measurement of *Syn* cells with or without pre-incubation with 5 mM NADP$^+$ for 0, 1, and 2 hr under continuous illumination. NADP$^+$ without cells (-*Syn*, black), *Syn* without NADP$^+$ (red), *Syn* after 0, 1, and 2 hr incubation with NADP$^+$ (blue, magenta, and green respectively).

(B) Calculations of the current sum that was accumulated during 10 min in CA measurements of NADP$^+$ without cells (-*Syn*, black), *Syn* without NADP$^+$ (red), *Syn* after 0, 1, and 2 hr incubation with NADP$^+$ (blue, magenta, and green respectively). The error bars represent the standard deviation over 3 independent measurements.

whether the ability to produce photocurrent by secretion of an endogenous electron mediator is specific to *Syn* or a more general phenomenon in cyanobacteria. In order to address this question, two additional cyanobacterial species were studied: *Acaryochloris marina MBIC 11017* (*Am*) and *Synechococcus elongatus* PCC 7942 (*Se*). Similar to *Syn*, the native habitat of *Se* is fresh water. However, *Se* has an elongated filament shape which is different than the round cells of *Syn*. The native habitat of *Am* is the oceanic salt water. Moreover, *Am* contains chl *d* which enables it to absorb wavelength beyond 700 nm for efficient photosynthesis.

2D-FMs of the ECMs of *Am* and *Se* after a 100 s of CA measurement in dark or under illumination were measured. NAD(P)H concentrations were calculated based on the fluorescence intensities and compared to standards of known concentrations. The results revealed that both strains exhibit light-induced accumulation of NAD(P)H in their ECM (Figure 7). In addition, the difference between light and dark incubation of both strains was similar to that shown for *Syn*.

As shown above for *Syn*, addition of exogenous NADP$^+$ or glucose significantly increases the photocurrent obtained from these two species (Figure S11). Addition of DCMU has a similar effect on the photocurrent than seen for *Syn*, while addition of FNR completely abrogates the photocurrent (Figure S11). Based on our findings and in agreement with our previous work (Saper et al., 2018), we suggest a model for the mechanism of the electron transport in the BPEC in which the electron source starts from the respiratory pathway and continues through the plastoquinone pool to PSI which reduces NADP$^+$ to NADPH. The link to the electrochemical component of the BPEC induces the release of NADPH, which reduces the anode and re-enters the cyanobacterial cell to accept additional electrons from PSI (Figure 8). Another minor electron donor is NADH which was also found to exit the cell and functions similar to NADPH. Several options exist for the final electron acceptor which is being reduced by the cathode: reduction of H^+ or water hydrolysis to form H_2, reduction of metabolites in the ECM, or direct reduction of the cells.

The actual capacity of photosynthetic organisms to perform efficient solar energy conversion has been a subject of debate for the past 20 years since the first studies of attempts to utilize photosynthesis (in the form of live cells, membranes, or isolated complexes) were reported. Comparisons with solid-state or dye-sensitized solar cells are seldom performed using the same metrics (Blankenship et al., 2011). Overall, photosynthetic efficiency is typically seen as low since much of the chemical output (in the form of sugars and ATP) goes toward cell growth and control. Comparison of PV-driven electrolysis vs. biomass production is for instance greatly in favor of PV. This of course does not take into account the energy expended in mining the raw materials (or used in their synthesis) or the carbon footprint of moving raw materials to sites of synthesis/assembly and transportation of completed panels to their site of use. When comparing pure quantum efficiency (photons absorbed to electrons transferred), PSII and PSI have been shown to be highly efficient comparable to photovoltaic/Dye-sensitized solar cells (PV/DSSC) devices. Translating the maximal

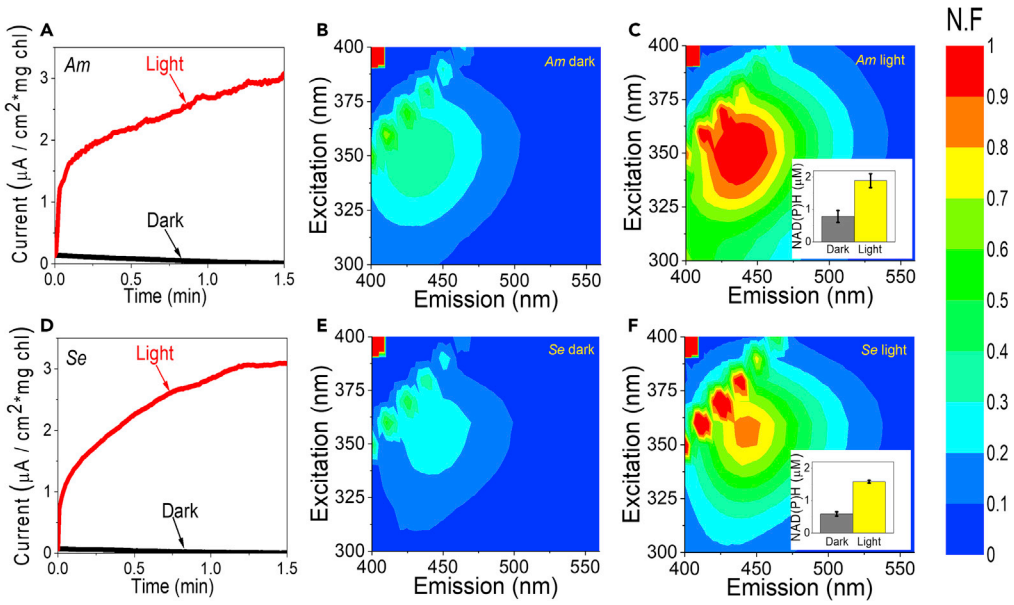

Figure 7. *Am* and *Se* exhibit light-driven current and export NADP(H) into the BPEC ECM similar to *Syn*

CA of *Am* and *Se* cells was measured for 100 s in dark and under illumination. The cells were filtrated immediately following the measurement, and 2D-FM spectra of their ECMs were measured.

(A) CA of *Am* cells in dark (black) and under illumination (red).

(B) 2D-FM spectra of the ECM of *Am* after measurements in dark.

(C) 2D-FM spectra of the ECM of *Am* after measurements under illumination.

(D) CA of *Se* cells in dark (black) and under illumination (red).

(E) 2D-FM spectra of the ECM of *Se* after measurements in dark.

(F) 2D-FM spectra of the ECM of *Se* after measurements under illumination. The inset in (C) and (F) displays NAD(P)H concentrations which were calculated based on the fluorescence intensities at (λ(ex) = 340 nm, λ(em) = 450 nm) after incubation in dark and under illumination. The error bars represent the standard deviation over 6 independent measurements. The fluorescence intensities in the color bar are displayed as normalized fluorescence (N.F).

electron flux through PSII (with water as the donor) or PSI (with a sacrificial electron donor), one can obtain sustained currents of 10-3000 mA mg chl^{-1} (depending on organism source and level of isolation) for saturating illumination in the range of 400-700 nm. Rates of PSI reduction of $NADP^+$ are comparable. We estimate that a two-dimensional 1 cm^2 solar panel based on photosynthetic material would require ~100 μg chl (in cells or thylakoid membranes) or about 10 μg chl (in isolated PSII/PSI) to operate. This is about the amount of material that can be isolated from a few spinach leaves or 1 gram (dry weight) of cyanobacterial cells. This current is on the same order of current that is obtained from commercial DSSC solar cells. Use of isolated components (membranes or complexes) requires systematic replacement due to irreparable damage due to photoinhibition but can provide elevated rates of electron transfer. Cells continually self-repair damaged systems; however, if dependent on the release of endogenous electron mediators, the currents will be an order of magnitude smaller. For this reason, we have identified the mediator to see if we can improve our BPEC that utilizes cells. Our identification of NADPH as a major mediating molecule is thus important since this natural molecule has many of the characteristics one would hope to use in a BPEC device: it is non-toxic, water soluble, redox active, and relatively stable. Developing methods where a single addition of $NADP^+$ to the ECM of a system based on live cells that can operate during a single day would be a tremendous advancement toward the future use of such a BPEC in the future for small-scale local solar energy conversion.

Limitations of the study

We show here that live cyanobacterial cells use endogenous NADPH as an electron mediator in a BPEC. NADPH is a redox active metabolite that is found in these cells at relatively high concentration (>15 nmol/mg chl) (Kauny and Sétif, 2014) and is continually produced by the coupled respiration and photosynthesis processes in active cells. Taken with our previous studies (Saper et al., 2018), these observations

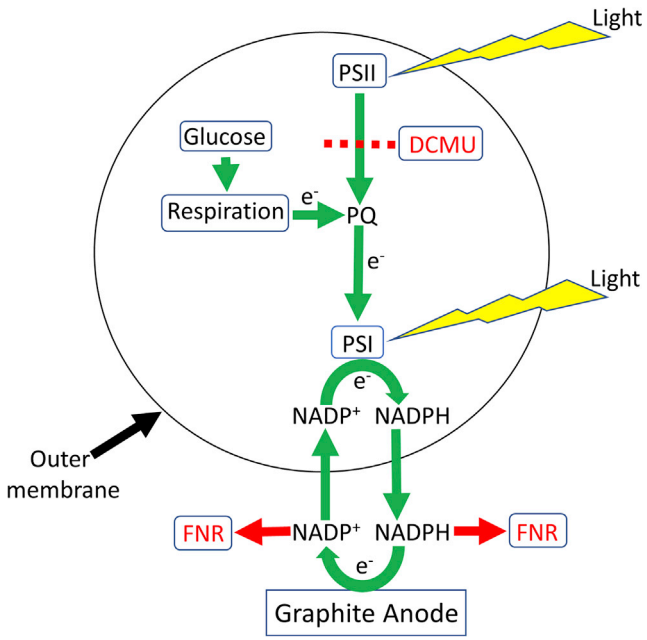

Figure 8. Schematic depiction of the main electron transport pathway in cyanobacterial BPECs

The electron transport originates from the respiratory pathway which reduces the PQ pool and continues downstream to PSI which under illumination reduces NADP + to NADPH. NADPH exits the stroma (cytoplasm) and outer membrane to the ECM and reduces the graphite anode. It then re-enters the cyanobacterial cells to accept more electrons from PSI. Yellow flash shapes indicate the light illumination which is absorbed in the photosystems. Green arrows represent the directionality of the electron transport pathway. Black arrows indicate the internal and outer cell membranes. A dashed line represents the electron blockage between PSII and the plastoquinone pool (PQ) in the presence of DCMU. Red arrows represent the binding of NADP+ and NADPH to exogenous FNR that prevent them from reducing the anode or re-entering the cell and in this manner abrogate the current production.

indicate that use of easily grown cells can provide current with the potential for either fuel (H_2) production or power storage for the entire length of a day without addition of polluting chemicals. In the future, we may see the production of sufficient energy to run a small local agricultural device using such a clean energy system; however, there are many technical obstacles, including the recycling of the live cells, maintaining such cultures during the night hours, and avoiding contaminations by other species.

Resource availability

Lead contact

Noam Adir (noam@ch.technion.ac.il)

Materials availability

Materials are available from the corresponding authors on request or are commercially available.

Data and code availability

This study did not generate computer code. All data and analytical methods are available in the main text or in Supplemental information section.

METHODS

All methods can be found in the accompanying Transparent Methods supplemental file.

SUPPLEMENTAL INFORMATION

Supplemental Information can be found online at https://doi.org/10.1016/j.isci.2020.101892.

ACKNOWLEDGMENTS

Funding for this study was provided by a "Nevet" grant from the Grand Technion Energy Program (GTEP) and a Technion VPR Berman Grant for Energy Research. Some of the results reported in this work were obtained using central facilities at the Technion's Hydrogen Technologies Research Laboratory (HTRL) supported by the Nancy & Stephen Grand Technion Energy Program (GTEP), the ADELIS Foundation, and the Solar Fuels I-CORE. We thank Dr. Yifat Nakibly for technical support. We thank Prof. Rachel Nechushtai and Prof. Iftach Yacoby for supplying biological materials. We thank Shira Bar-Zvi, Sonya Copperstein, and Lee Keysar for their assistance. Y.S. and T.üN.T.ó are supported by fellowships of the Nancy & Stephen Grand Technion Energy Program (GTEP) and by a Schulich Graduate fellowship.

AUTHORS CONTRIBUTION

Y.S., G.S., and N.A. conceived the idea. Y.S., G.S., and N.A. designed the experiments. Y.S. performed the main experiments. B.E., T.N.T., and G.L. assisted in performing the experiments. Y.S., G.S., and N.A. wrote the paper. G.S. and N.A. supervised, administrated, and acquired the funding for the entire research.

DECLARATION OF INTERESTS

The authors declare no competing interests.

Received: September 16, 2020
Revised: October 31, 2020
Accepted: December 1, 2020
Published: January 22, 2021

REFERENCES

Batie, C.J., and Kamin, H. (1986). Association of ferredoxin-NADP+ reductase with NADP(H) specificity and oxidation-reduction properties. J. Biol. Chem. *261*, 11214–11223.

Bergel, A., Féron, D., and Mollica, A. (2005). Catalysis of oxygen reduction in PEM fuel cell by seawater biofilm. Electrochem. Commun. *7*, 900–904.

Blacker, T.S., Mann, Z.F., Gale, J.E., Ziegler, M., Bain, A.J., Szabadkai, G., and Duchen, M.R. (2014). Separating NADH and NADPH fluorescence in live cells and tissues using FLIM. Nat. Commun. *5*, 3936.

Blankenship, R.E., Tiede, D.M., Barber, J., Brudvig, G.W., Fleming, G., Ghirardi, M., Gunner, M.R., Junge, W., Kramer, D.M., Melis, A., et al. (2011). Comparing photosynthetic and photovoltaic efficiencies and recognizing the potential for improvement. Science *332*, 805–809.

Bombelli, P., Müller, T., Herling, T.W., Howe, C.J., and Knowles, T.P.J. (2015). A high power-density, mediator-free, microfluidic biophotovoltaic device for cyanobacterial cells. Adv. Energy Mater. *5*, 1–6.

Bond, D.R., Holmes, D.E., Tender, L.M., and Lovley, D.R. (2002). Electrode-reducing microorganisms that harvest energy from marine sediments *295*, 483–485.

Bond, D.R., and Lovley, D.R. (2003). Electricity production by Geobacter sulfurreducens attached to electrodes. Appl. Environ. Microbiol. *69*, 1548–1555.

Calkins, J.O., Umasankar, Y., O'Neill, H., and Ramasamy, R.P. (2013). High photo-electrochemical activity of thylakoid–carbon nanotube composites for photosynthetic energy conversion. Energy Environ. Sci. *6*, 1891–1900.

Cereda, A. (2014). A bioelectrochemical approach to characterize extracellular electron transfer by Synechocystis sp. PCC6803. PLoS One *9*, e91484.

Chaudhuri, S.K., and Lovley, D.R. (2003). Electricity generation by direct oxidation of glucose in mediatorless microbial fuel cells. Nat. Biotechnol. *21*, 1229–1232.

Choi, Y., Jung, E., Kim, S., and Jung, S. (2003). Membrane fluidity sensoring microbial fuel cell. Bioelectrochemistry *59*, 121–127.

Dartnell, L.R., Storrie-Lombardi, M.C., and Ward, J.M. (2010). Complete fluorescent fingerprints of extremophilic and photosynthetic microbes. Int. J. Astrobiol. *9*, 245–257.

Deng, M.D., and Coleman, J.R. (1999). Ethanol synthesis by genetic engineering in cyanobacteria. Appl. Environ. Microbiol. *65*, 523–528.

Efrati, A., Lu, C.H., Michaeli, D., Nechushtai, R., Alsaoub, S., Schuhmann, W., and Willner, I. (2016). Assembly of photo-bioelectrochemical cells using photosystem I-functionalized electrodes. Nat. Energy *1*, 1–7, 15021.

Efrati, A., Tel-Vered, R., Michaeli, D., Nechushtai, R., and Willner, I. (2013). Cytochrome c-coupled photosystem I and photosystem II (PSI/PSII) photo-bioelectrochemical cells. Energy Environ. Sci. *6*, 2950–2956.

Fang, X., Kalathil, S., and Reisner, E. (2020). Semi-biological approaches to solar-to-chemical conversion. Chem. Soc. Rev. *49*, 4926–4952.

Gizzie, E.A., Niezgoda, J.S., Robinson, M.T., Harris, A.G., Jennings, G.K., Rosenthala, S.J., and Cliffel, D.E. (2015). Photosystem I-polyaniline/TiO2 solid-state solar cells: simple devices for biohybrid solar energy conversion. Energy Environ. Sci. *8*, 3572–3576.

Grattieri, M. (2020). Purple bacteria photo-bioelectrochemistry: enthralling challenges and opportunities. Photochem. Photobiol. Sci. *19*, 424–435.

Grattieri, M., Beaver, K., Gaffney, E.M., and Minteer, S.D. (2019a). Tuning purple bacteria salt-tolerance for photobioelectrochemical systems in saline environments. Faraday Discuss *215*, 15–25.

Grattieri, M., Rhodes, Z., Hickey, D.P., Beaver, K., and Minteer, S.D. (2019b). Understanding biophotocurrent generation in photosynthetic purple bacteria. ACS Catal. *9*, 867–873.

Gruber, A., and Haferkamp, I. (2019). Nucleotide transport and metabolism in diatoms. Biomolecules *9*, 761.

Gregory, K.B., Bond, D.R., and Lovley, D.R. (2004). Graphite electrodes as electron donors for anaerobic respiration. Environ. Microbiol. *6*, 596–604.

Hartmann, V., Harris, D., Bobrowski, T., Ruff, A., Frank, A., Günther Pomorski, T., Rögner, M., Schuhmann, W., Adir, N., and Nowaczyk, M.M. (2020). Improved quantum efficiency in an engineered light harvesting/photosystem II super-complex for high current density biophotoanodes. J. Mater. Chem. A. *8*, 14463–14471.

Hartshorne, R.S., Jepson, B.N., Clarke, T.A., Field, S.J., Fredrickson, J., Zachara, J., Shi, L., Butt, J.N., and Richardson, D.J. (2007). Characterization of

Shewanella oneidensis MtrC: a cell-surface decaheme cytochrome involved in respiratory electron transport to extracellular electron acceptors. J. Biol. Inorg. Chem. *12*, 1083–1094.

Hasan, K., Milton, R.D., Grattieri, M., Wang, T., Stephanz, M., and Minteer, S.D. (2017). Photobioelectrocatalysis of intact chloroplasts for solar energy conversion. ACS Catal. *7*, 2257–2265.

Heidary, N., Kornienko, N., Kalathil, S., Fang, X., Ly, K.H., Greer, H.F., and Reisner, E. (2020). Disparity of cytochrome utilization in anodic and cathodic extracellular electron transfer pathways of Geobacter sulfurreducens biofilms. J. Am. Chem. Soc. *142*, 5194–5203.

Huang, L.F., Lin, J.Y., Pan, K.Y., Huang, C.K., and Chu, Y.K. (2015). Overexpressing ferredoxins in Chlamydomonas reinhardtii increase starch and oil yields and enhance electric power production in a photo microbial fuel cell. Int. J. Mol. Sci. *16*, 19308–19325.

Ieropoulos, I., Greenman, J., Melhuish, C., and Hart, J. (2005). Comparative study of three types of microbial fuel cell. Enzyme Microb. Technol. *37*, 238–245.

Kaiser, B.K., Carleton, M., Hickman, J.W., Miller, C., Lawson, D., Budde, M., Warrener, P., Paredes, A., Mullapudi, S., Navarro, P., et al. (2013). Fatty aldehydes in cyanobacteria are a metabolically flexible precursor for a diversity of biofuel products. PLoS One *8*, e58307.

Kauny, J., and Sétif, P. (2014). NADPH fluorescence in the cyanobacterium Synechocystis sp. PCC 6803: a versatile probe for in vivo measurements of rates, yields and pools. Biochim. Biophys. Acta *1837*, 792–801.

Keren, N., Kidd, M.J., Penner-Hahn, J.E., and Pakrasi, H.B. (2002). A light-dependent mechanism for massive accumulation of manganese in the photosynthetic bacterium Synechocystis sp. PCC 6803. Biochemistry *41*, 15085–15092.

Kim, B.H., Kim, H.J., Hyun, M.S., and Park, D.H. (1999). Direct electrode reaction of Fe(III)-reducing bacterium, Shewanella putrefaciens. J. Microbiol. Biotechnol. *9*, 127–131.

Kowata, H., Tochigi, S., Takahashi, H., and Kojima, S. (2017). Outer membrane permeability of cyanobacterium Synechocystis sp. strain PCC 6803: studies of passive diffusion of small organic nutrients reveal the absence of classical porins and intrinsically low permeability. J. Bacteriol. *199*, e00371–17.

Kranzler, C., Lis, H., Finkel, O.M., Schmetterer, G., Shaked, Y., and Keren, N. (2014). Coordinated transporter activity shapes high-affinity iron acquisition in cyanobacteria. ISME J. *8*, 409–417.

Lan, J.C.W., Raman, K., Huang, C.M., and Chang, C.M. (2013). The impact of monochromatic blue and red LED light upon performance of photo microbial fuel cells (PMFCs) using Chlamydomonas reinhardtii transformation F5 as biocatalyst. Biochem. Eng. J. *78*, 39–43.

Laohavisit, A., Anderson, A., Bombelli, P., Jacobs, M., Howe, C.J., Davies, J.M., and Smith, A.G. (2015). Enhancing plasma membrane NADPH oxidase activity increases current output by diatoms in biophotovoltaic devices. Algal Res. *12*, 91–98.

Larom, S., Kallmann, D., Saper, G., Pinhassi, R., Rothschild, A., Dotan, H., Ankonina, G., Schuster, G., and Adir, N. (2015). The Photosystem II D1-K238E mutation enhances electrical current production using cyanobacterial thylakoid membranes in a bio-photoelectrochemical cell. Photosynth. Res. *126*, 161–169.

Larom, S., Salama, F., Schuster, G., and Adir, N. (2010). Engineering of an alternative electron transfer path in photosystem II. Proc. Natl. Acad. Sci. *107*, 9650–9655.

Lawaetz, A.J., and Stedmon, C.A. (2009). Fluorescence intensity calibration using the Raman scatter peak of water. Appl. Spectrosc. *63*, 936–940.

Lee, S.A., Choi, Y., Jung, S., and Kim, S. (2002). Effect of initial carbon sources on the electrochemical detection of glucose by Gluconobacter oxydans. Bioelectrochemistry *57*, 173–178.

Li, J., Feng, X., Fei, J., Cai, P., Huang, J., and Li, J. (2016). Integrating photosystem II into a porous TiO2 nanotube network toward highly efficient photo-bioelectrochemical cells. J. Mater. Chem. A. *4*, 12197–12204.

Liu, Z.D., Lian, J., Du, Z.W., and Li, H.R. (2006). Construction of sugar-based microbial fuel cells by dissimilatory metal reduction bacteria. Chin. J. Biotechnol. *22*, 131–137.

Longatte, G., Sayegh, A., Delacotte, J., Rappaport, F., Wollman, F.A., Guille-Collignon, M., and Lemaître, F. (2018). Investigation of photocurrents resulting from a living unicellular algae suspension with quinones over time. Chem. Sci. *9*, 8271–8281.

Lovley, D.R. (2012). Electromicrobiology. Annu. Rev. Microbiol. *66*, 391–409.

Lovley, D.R., Coates, J.D., Blunt-Harris, E.L., Phillips, E.J.P., and Woodward, J.C. (1996). Humic substances as electron acceptors for microbial respiration. Nature *382*, 445–448.

Lovley, D.R., Holmes, D.E., and Nevin, K.P. (2004). Dissimilatory Fe(III) and Mn(IV) reduction. Adv. Microb. Physiol. *49*, 219–286.

Major, P., Embley, T.M., and Williams, T.A. (2017). Phylogenetic diversity of NTT nucleotide transport proteins in free-living and parasitic bacteria and Eukaryotes. Genome Biol. Evol. *9*, 480–487.

McCormick, A.J., Bombelli, P., Bradley, R.W., Thorne, R., Wenzele, T., and Howe, C.J. (2015). Biophotovoltaics: oxygenic photosynthetic organisms in the world of bioelectrochemical systems. Energy Environ. Sci. *8*, 1092–1109.

McCormick, A.J. (2013). Hydrogen production through oxygenic photosynthesis using the cyanobacterium Synechocystis sp. PCC 6803 in a bio-photoelectrolysis cell (BPE) system. Energy Environ. Sci. *6*, 2682–2690.

McCormick, A.J., Bombelli, P., Scott, A.M., Philips, A.J., Smith, A.G., Fisher, A.C., and Howe, C.J. (2011). Photosynthetic biofilms in pure culture harness solar energy in a mediatorless bio-photovoltaic cell (BPV) system. Energy Environ. Sci. *4*, 4699–4709.

Menicucci, J., Beyenal, H., Marsili, E., Veluchamy, Demir G., and Lewandowski, Z. (2006). Procedure for determining maximum sustainable power generated by microbial fuel cells. Environ. Sci. Technol. *40*, 1062–1068.

Mershin, A., Matsumoto, K., Kaiser, L., Yu, D., Vaughn, M., Nazeeruddin, M.K., Bruce, B.D., Graetzel, M., and Zhang, F. (2012). Self-assembled photosystem-I biophotovoltaics on nanostructured TiO2 and ZnO. Sci. Rep. *2*, 234.

Min, B., Cheng, S., and Logan, B.E. (2005). Electricity generation using membrane and salt bridge microbial fuel cells. Water Res. *39*, 1675–1686.

Murakawa, S., and Takahashi, T. (1978). Stimulation of glutamate uptake by NADH and NADPH in intact cells of Escherichia coli mutant defective in Mg2+, Ca2+-ATPase. Agric. Biol. Chem. *42*, 1803–1804.

Nevin, K.P., Richter, H., Covalla, S.F., Johnson, J.P., Woodard, T.L., Orloff, A.L., Jia, H., Zhang, M., and Lovley, D.R. (2008). Power output and columbic efficiencies from biofilms of Geobacter sulfurreducens comparable to mixed community microbial fuel cells. Environ. Microbiol. *10*, 2505–2514.

Ochiai, H., Shibata, H., Sawa, Y., Shoga, M., and Ohta, S. (1983). Properties of semiconductor electrodes coated with living films of cyanobacteria. Appl. Biochem. Biotechnol. *8*, 289–303.

Park, D., and Zeikus, J. (2002). Impact of electrode composition on electricity generation in a single-compartment fuel cell using Shewanella putrefaciens. Appl. Microbiol. Biotechnol. *59*, 58–61.

Park, D.H., Laivenieks, M., Guettler, M.V., Jain, M.K., and Zeikus, J.G. (1999). Microbial utilization of electrically reduced neutral red as the sole electron donor for growth and metabolite production. Appl. Environ. Microbiol. *65*, 2912–2917.

Park, D.H., and Zeikus, J.G. (2000). Electricity generation in microbial fuel cells using neutral red as an electronophore. Appl. Environ. Microbiol. *66*, 1292–1297.

Park, D.H., and Zeikus, J.G. (1999). Utilization of electrically reduced neutral red by Actinobacillus succinogenes: physiological function of neutral red in membrane-driven fumarate reduction and energy conservation. J. Bacteriol. *181*, 2403–2410.

Pham, C.A., Jung, S.J., Phung, N.T., Lee, J., Chang, I.S., Kim, B.H., Yi, H., and Chun, J. (2003). A novel electrochemically active and Fe(III)-reducing bacterium phylogenetically related to Aeromonas hydrophila, isolated from a microbial fuel cell. FEMS Microbiol. Lett. *223*, 129–134.

Pinhassi, R.I., Kallmann, D., Saper, G., Dotan, H., Linkov, A., Kay, A., Liveanu, V., Schuster, G., Adir, N., and Rothschild, A. (2016). Hybrid bio-photo-electro-chemical cells for solar water splitting. Nat. Commun. *7*, 12552.

Pinhassi, R.I., Kallmann, D., Saper, G., Larom, S., Linkov, A., Boulouis, A., Schöttler, M.A., Bock, R.,

Rothschild, A., Adir, N., and Schuster, G. (2015). Photosynthetic membranes of Synechocystis or plants convert sunlight to photocurrent through different pathways due to different architectures. PLoS One *10*, e0122616.

Rabaey, K., Boon, N., Höfte, M., and Verstraete, W. (2005). Microbial phenazine production enhances electron transfer in biofuel cells. Environ. Sci. Technol. *39*, 3401–3408.

Rabaey, K., Boon, N., Siciliano, S.D., Verhaege, M., and Verstraete, W. (2004). Biofuel cells select for microbial consortia that self-mediate electron transfer. Appl. Environ. Microbiol. *70*, 5373–5382.

Rhoads, A., Beyenal, H., and Lewandowski, Z. (2005). Microbial fuel cell using anaerobic respiration as an anodic reaction and biomineralized manganese as a cathodic reactant. Environ. Sci. Technol. *39*, 4666–4671.

Ringeisen, B.R., Henderson, E., Wu, P.K., Pietron, J., Ray, R., Little, B., Biffinger, J.C., and Jones-Meehan, J.M. (2006). High power density from a miniature microbial fuel cell using Shewanella oneidensis DSP10. Environ. Sci. Technol. *40*, 2629–2634.

Saper, G., Kallmann, D., Conzuelo, F., Zhao, F., Tóth, T.N., Liveanu, V., Meir, S., Szymanski, J., Aharoni, A., Schuhmann, W., et al. (2018). Live cyanobacteria produce photocurrent and hydrogen using both the respiratory and photosynthetic systems. Nat. Commun. *9*, 2168.

Sawa, M., Fantuzzi, A., Bombelli, P., Howe, C.J., Hellgardt, K., and Nixon, P.J. (2017). Electricity generation from digitally printed cyanobacteria. Nat. Commun. *8*, 1327.

Schmetterer, G., Alge, D., and Gregor, W. (1994). Deletion of cytochrome c oxidase genes from the cyanobacterium Synechocystis sp. PCC6803: evidence for alternative respiratory pathways. Photosynth. Res. *42*, 43–50.

Sekar, N., Jain, R., Yan, Y., and Ramasamy, R.P. (2016). Enhanced photo-bioelectrochemical energy conversion by genetically engineered cyanobacteria. Biotechnol. Bioeng. *113*, 675–679.

Sekar, N., Umasankar, Y., and Ramasamy, R.P. (2014). Photocurrent generation by immobilized cyanobacteria via direct electron transport in photo-bioelectrochemical cells. Phys. Chem. Chem. Phys. *16*, 7862–7871.

Shi, L., Rosso, K.M., Zachara, J.M., and Fredrickson, J.K. (2012). Mtr extracellular electron-transfer pathways in Fe(III)-reducing or Fe(II)-oxidizing bacteria: a genomic perspective. Biochem. Soc. Trans. *40*, 1261–1267.

Simoska, O., Sans, M., Eberlin, L.S., Shear, J.B., and Stevenson, K.J. (2019). Electrochemical monitoring of the impact of polymicrobial infections on Pseudomonas aeruginosa and growth dependent medium. Biosens. Bioelectron. *142*, 111538.

Stingaciu, L.R., O'Neill, H.M., Liberton, M., Pakrasi, H.B., and Urban, V.S. (2019). Influence of chemically disrupted photosynthesis on cyanobacterial thylakoid dynamics in Synechocystis sp. PCC 6803. Sci. Rep. *9*, 5711.

Tanaka, K., Kashiwagi, N., and Ogawa, T. (1988). Effects of light on the electrical output of bioelectrochemical fuel-cells containing Anabaena variabilis M-2: mechanism of the post-illumination burst. J. Chem. Technol. Biotechnol. *42*, 235–240.

Tanaka, K., Tamamushi, R., and Ogawa, T. (1985). Bioelectrochemical fuel-cells operated by the cyanobacterium, anabaena variabilis. J. Chem. Technol. Biotechnol. Biotechnol. *35 B*, 191–197.

Tanaka, K., Vega, C., and Tamamushi, R. (1983). Mediating effects of ferric chelate compound in microbial fuel cells. J. Electroanal. Chem. *156*, 135–143.

Thirumurthy, M.A., Hitchcock, A., Cereda, A., Liu, J., Chavez, M.S., Doss, B.L., Ros, R., El-Naggar, M.Y., Heap, J.T., Bibby, T.S., et al. (2020). Type IV pili-independent photocurrent production by the cyanobacterium synechocystis sp. PCC 6803. Front. Microbiol. *11*, 1344.

Thurston, C.F., Bennetto, H.P., and Delaney, G.M. (1985). Glucose metabolism in a microbial fuel cell. Stoichiometry of product formation in a thionine-mediated Proteus vulgaris fuel cell and its relation to coulombic yields. J. Gen. Microbiol. *131*, 1393–1401.

Torimura, M., Miki, A., Wadano, A., Kano, K., and Ikeda, T. (2001). Electrochemical investigation of cyanobacteria Synechococcus sp. PCC7942-catalyzed photoreduction of exogenous quinones and photoelectrochemical oxidation of water. J. Electroanal. Chem. *496*, 21–28.

Tschörtner, J., Lai, B., and Krömer, J.O. (2019). Biophotovoltaics: green power generation from sunlight and water. Front. Microbiol. *10*, 866.

U.S. IEA (2011). Annual Energy Outlook 2011.

Vaara, M. (1992). Agents that increase the permeability of the outer membrane. Microbiol. Rev. *56*, 395–411.

Wei, X., Lee, H., and Choi, S. (2016). Biopower generation in a microfluidic bio-solar panel. Sens. Actuators B Chem. *228*, 151–155.

Yagishita, T., Horigome, T., and Tanaka, K. (1993). Effects of light, CO2 and inhibitors on the current output of biofuel cells containing the photosynthetic organism Synechococcus sp. J. Chem. Technol. Biotechnol. *56*, 393–399.

Yehezkeli, O., Tel-Vered, R., Wasserman, J., Trifonov, A., Michaeli, D., Nechushtai, E., and Willner, I. (2012). Integrated photosystem II-based photo-bioelectrochemical cells. Nat. Commun. *3*, 742.

Yi, H., Nevin, K.P., Kim, B.C., Franks, A.E., Klimes, A., Tender, L.M., and Lovley, D.R. (2009). Selection of a variant of Geobacter sulfurreducens with enhanced capacity for current production in microbial fuel cells. Biosens. Bioelectron. *24*, 3498–3503.

Zhang, L., Selão, T.T., Pisareva, T., Qian, J., Sze, S.K., Carlberg, I., and Norling, B. (2013). Deletion of Synechocystis sp. PCC 6803 leader peptidase LepB1 affects photosynthetic complexes and respiration. Mol. Cell. Proteomics *12*, 1192–1203.

Zhao, F., Conzuelo, F., Hartmann, V., Li, H., Nowaczyk, M.M., Plumeré, N., Rögner, M., and Schuhmann, W. (2015). Light induced H2 evolution from a biophotocathode based on photosystem 1–Pt nanoparticles complexes integrated in solvated redox polymers films. J. Phys. Chem. B. *119*, 13726–13731.

Zhao, F., Sliozberg, K., Rögner, M., Plumeré, N., and Schuhmann, W. (2014). The role of hydrophobicity of Os-complex-modified polymers for photosystem 1 based photocathodes. J. Electrochem. Soc. *161*, H3035–H3041.

Zhou, Y., Wang, L., Yang, F., Lin, X., Zhang, S., and Zhao, Z.K. (2011). Determining the extremes of the cellular NAD(H) level by using an Escherichia coli NAD+-auxotrophic mutant. Appl. Environ. Microbiol. *77*, 6133–6140.

Zou, Y., Pisciotta, J., and Baskakov, I.V.((2010). Nanostructured polypyrrole-coated anode for sun-powered microbial fuel cells. Bioelectrochemistry *79*, 50–56.

Zou, Y., Pisciotta, J., Billmyre, R.B., and Baskakov, I.V.((2009). Photosynthetic microbial fuel cells with positive light response. Biotechnol. Bioeng. *104*, 939–946.

iScience, Volume *24*

Supplemental Information

NADPH performs mediated electron transfer in cyanobacterial-driven bio-photoelectrochemical cells

Yaniv Shlosberg, Benjamin Eichenbaum, Tünde N. Tóth, Guy Levin, Varda Liveanu, Gadi Schuster, and Noam Adir

Supplementary Information

NADPH performs mediated electron transfer in cyanobacterial-driven bio-photoelectrochemical cells

Yaniv Shlosberg[1,2], Benjamin Eichenbaum[3], Tünde N. Tóth[1,2], Guy Levin[3] Varda Liveanu[3], Gadi Schuster[*,1,3] and Noam Adir[*,1,2].

Transparent methods

Materials

All chemicals were purchased from Merck unless mentioned otherwise.

Millipore hydrophilic PVDF filter Membrane 0.22 μm were purchased from Millex-HV.

Two different Ferredoxin $NADP^+$ Reductase (FNR) proteins were used in this work. The first (mcFNR) was isolated from thermophilic cyanobacteria *Mastigocladus laminosus* and kindly obtained from Prof. Rachel Nechushtai, the Hebrew University of Jerusalem (Fish et al., 2003). The second (crFNR) was produced in *E. coli* using an expression plasmid harbouring the *Chlamydomonas reinhrdtii* FNR cDNA, kindly provided by Prof. Iftach Yacoby at Tel Aviv University. crFNR was purified (Marco et al., 2019).

Species cultivation

Synechocystis sp. PCC6803 (*Syn*) and *Synechococcus elongatus* PCC 7942 (*Se*) were cultivated in BG11 medium in growth chamber at light intensity of about 100 μE / m^2 s, shaking at 100 rpm and at $29C^0$. *Acaryochloris marina MBIC 11017* (*Am*) was cultivated in MBG11 media (a BG11 medium containing 30 g/L sea salts (Instant Ocean) (Bar-Zvi et al., 2018).

Samples preparation

O.D measurements of the cells was done at 750 nm (Nanodrop 2000 UV-Vis spectrophotometer, Thermo Fisher Scientific). Cell count was done under the microscope using a haemocytometer grid. For the measurements in the BPEC, log phase grown cells ($O.D_{750nm}$ = 0.6 – 1.0) were centrifuged (Multifuge X1R, Thermoscientific) for 10 min at 7500 rpm. The supernatant was removed, and the pellet was resuspended in a solution of MES buffer (MES 50 mM (pH=6), 10 mM NaCl, 5 mM MgCl. Optimization experiments showed that while pH=6.0 gave the highest photocurrent values, measurements could be done with only small changes in the range of pH = 5-8 (Fig. S12).

Chlorophyll concentration was determined by 90% methanol extraction followed by absorption measurements at 665 nm for chl a and 696 nm for chl d. Calculation of Chl concentration was performed as previously described (Ritchie, 2008, 2006). For use in the BPEC, live cyanobacterial cells were diluted in MES buffer solution to have a final concentration of 0.1 mg/mL total chl. The cells were allowed to precipitate for 0.5 minute prior to initiating CA measurements.

Chronoamperometry measurements

Chronoamperometry measurements were done using Plamsens3 potentiostat (Palmsens) connected to screen printed electrodes (AC1.W4.R1, BVT technologies). The WE has a surface area of 0.79 mm^2 and the distances between electrodes are: 1.95 mm (WE-CE), 0.68 mm (WE-RE) and 0.25 mm (CE-RE) Illumination of 1.5 SUN (calibrated at the electrode surface height without samples) was done using a solar simulator (Abet). In all measurements, a bias potential of 0.5 was applied on the graphite anode (this bias value was chosen because it produced the maximal signal / noise in the CA measurements). Total current calculations were done by summing all current values of the measurement which were acquired in time steps of 0.5 s. The volume of all measured samples was 50 µL that were pipetted directly on to the printed electrodes panel. The round boundaries of the measuring area of the panel induced a similar drop shape in all measurements that did not leak to the sides by surface tension of the liquid. The drop was not stirred and the cells typically do not sediment spontaneously over the short measurement duration of 3-10 min. As preparation for fluorescence measurements, 50 µL of bacterial cells were filtrated through a 0.22 µm filter membrane to produce the ECM solution. each sample was diluted with fresh BPEC buffer to a final volume of 2 mL.

Fluorescence measurements

All fluorescence measurements, unless mentioned otherwise indicated, were done using a Fluorolog 3 fluorimeter (Horiba) with excitation and emission slits bands of 4 nm. Quantification of NAD(P)H concentrations were calculated based on NADH calibration curve which was based on increasing concentrations measured at (λ(ex) = 350 nm, λ(em) = 450 nm). The lines of diagonal spots that appear in all of the maps presented here and in the following figures results from light scattering of the Xenon lamp and Raman scattering of the water (Lawaetz and Stedmon, 2009).

Selective quantification of NADH and NADPH.

Selective quantification of NADH was done using NAD^+/NADH Quantification Kit (Cat. #MAK037, Sigma). Quantification of NADPH was done using a $NADP^+$/NADPH Assay Kit (Cat. #MAK312, Sigma). Briefly, in both kits 50 µL of *Syn* ECM was incubated with 50 µL enzymatic probes for specific detection of NADH or NADPH. Each sample was analysed in 9 replicates (each in a different well) in 96 wells plates. Triplicates of 5 different known NADH and NADPH increasing concentrations were incubated in the same plates for the construction of calibration curves.

Absorption for NADH quantification (450 nm) or fluorescence for NADPH quantification (ex = 530 nm / em = 585 nm) were measured using Spectramax M2 plate reader (Molecular Devices). Concentrations were determined based on the calibration curves which were plotted based on the known concentration of standards.

Supplemental Data

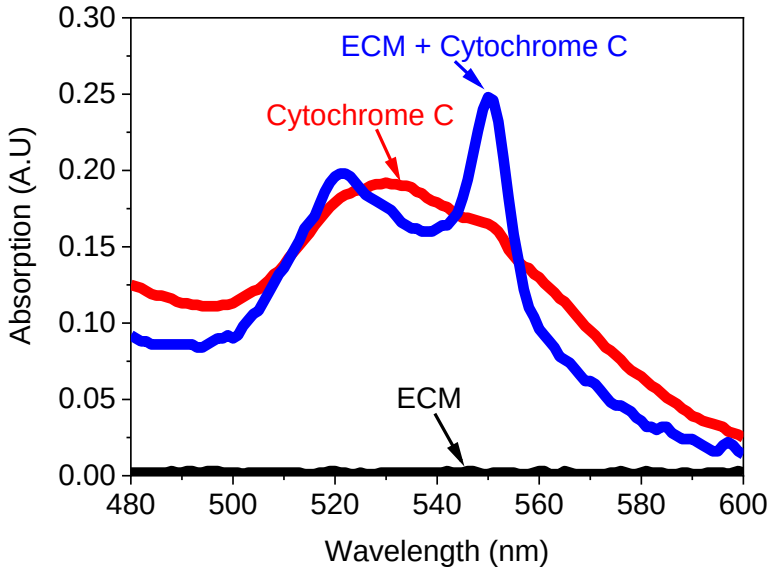

Fig. S1 - Following incubation of *Syn* in the BPEC, the ECM reduces Cytochrome C, Related to Fig. 1.

In order to show that the ECM of *Syn* contains reducing agents, absorption spectra of the ECM (black), oxidized Cytochrome C (red) and a mixture of ECM + Cytochrome C (blue) were measured after 20 min incubation. The observed spectral split from a single peak into 2 peaks in the mixture indicates the reduction of Cytochrome C by the ECM solution.

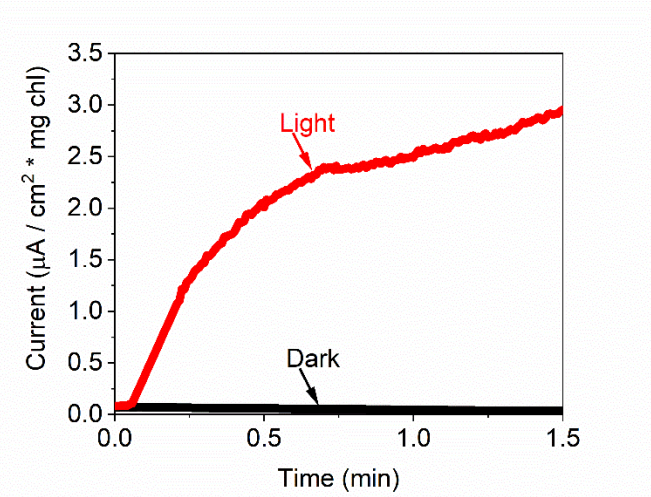

Fig. S2 – *Syn* do not produce current in dark, Related to Fig. 1. CA measurements of *Syn* in dark and light was performed to investigate whether some of the electrical current may be formed without any connection to photosynthesis. No current was obtained in dark. CA of *Syn* in dark (black). CA of *Syn* in light (red).

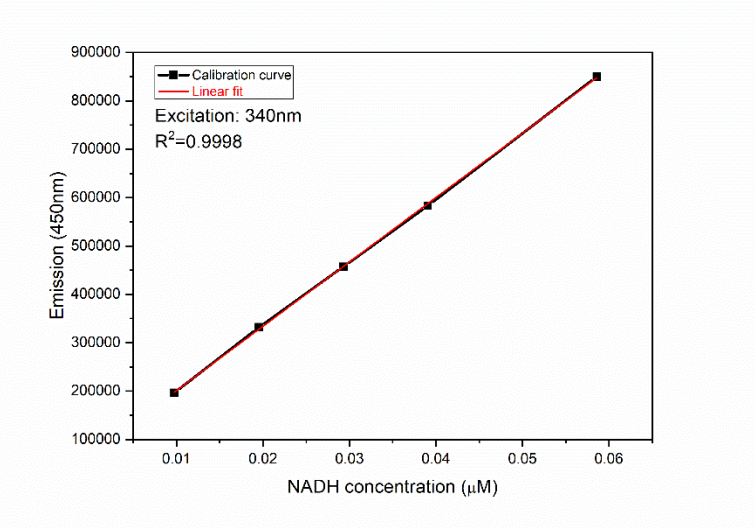

Fig. S3 - Calibration curve of NADH concentration vs. fluorescence intensity, Related to Fig. 2.
Fluorescence intensities was plotted against several NADH concentrations (λ(ex) = 350, λ(em) = 450 nm) (black). Linear fitting analysis (red). ECM samples with a volume of 50 µL after or not after CA measurements were diluted to a final volume of 2 mL (in order to have enough volume for the measurement) and their original concentrations were determined based on the curve and the dilution factor.

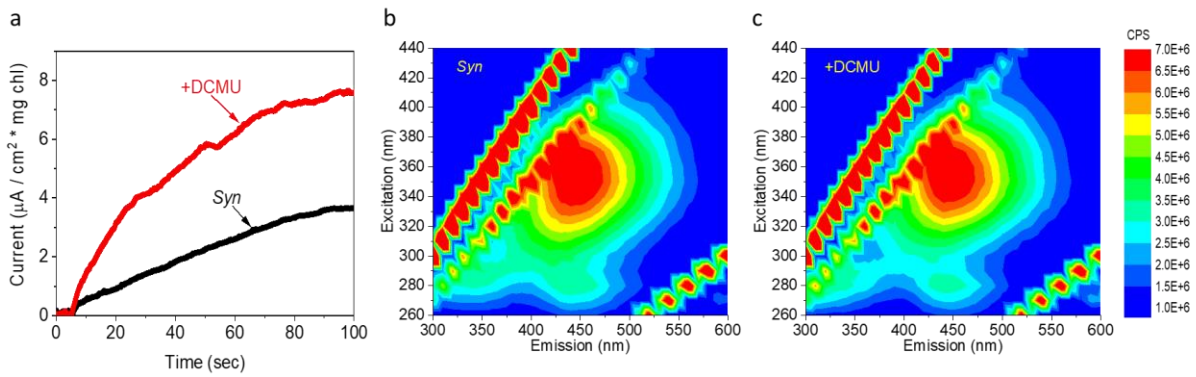

Fig. S4 – DCMU increases the photocurrent production, Related to Fig. 3. A. The herbicide DCMU was previously shown to increase the photocurrent.[1] Addition of 200 µM DCMU to *Syn* in the miniBPEC described here showed about 2-fold increase in current. **b and c.** 2D-FM of the ECM of *Syn* after CA measurement of *Syn* cells in the absence (**b)** or presence (**c**) of DCMU after 100 sec. of BPEC operation.

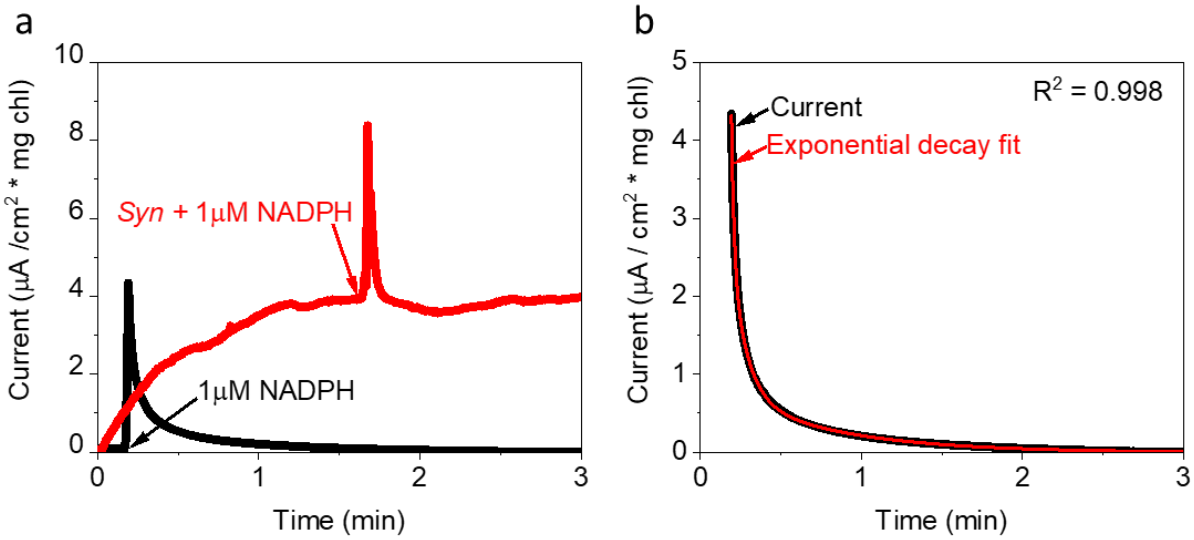

Fig. S5 - Addition of exogenous NADPH to the BPEC with or without *Syn* cells, Related to Figs. 3, 4 and 6. In order to estimate the ability of exogenous NADPH to produce photocurrent in the BPEC, 1 μM NADPH was added with or without *Syn* cells. In both measurements a fast increase of about 4 μA was obtained followed by a fast decrease of the current to the same level as it was prior to the addition within a few seconds. The fast current decay suggests that in order to maintain the current cyanobacteria needs to continuously secrete NADPH to the ECM. 1 μM NADPH was added to the BPEC in the absence of *Syn* cells (black) and in the presence of *Syn* measurement after the current reaches it maxima at 1.6 min (red). Arrows indicate the time point of NADPH addition.

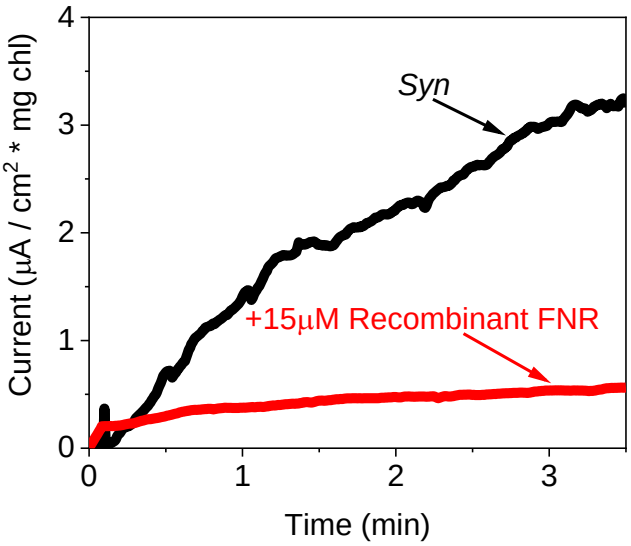

Fig. S6 - CA of *Syn* was measured with or without addition of 15μM recombinant FNR enzyme whose plasmid origin is *Chlamydomonas*, Related to Fig. 5. To strengthen the previous results that showed that addition of FNR isolated from thermophilic cyanobacteria *Mastigocladus laminosus* to *Syn* abrogates the photocurrent, we wished to repeat the same experiment with FNR from additional origin. For this purpose, CA of *Syn* with or without 15 μM of the recombinant FNR enzyme whose plasmid origin is from the green algae

Chlamydomonas reinhardtii was measured. Addition of the recombinant FNR has also abrogated the photocurrent. *Syn* (black), *Syn* + 15 µM FNR (red).

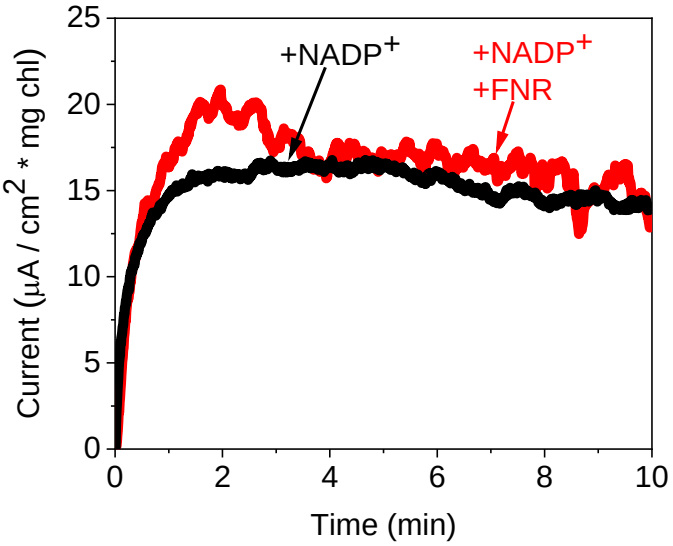

Fig. S7 - Addition of FNR in the presence of $NADP^+$ with a significantly higher concentration do not abrogate the current, Related to Fig. 5. CA of *Syn* + 5 mM $NADP^+$ (after 2 h incubation) was measured in with or without 30 µM FNR **(**from thermophilic cyanobacteria *M. laminosus*). No significant difference was observed between the 2 measurements. This finding indicates that in the presence of such $NADP^+$ concentration which is 3 magnitudes higher than FNR, all the FNR is bound. Therefore, it cannot bind to NADPH molecules that the cells secrete and do not abrogate the photocurrent production. *Syn* + 5 mM $NADP^+$ (black). *Syn* + 5 mM $NADP^+$ + 30 µM FNR (red).

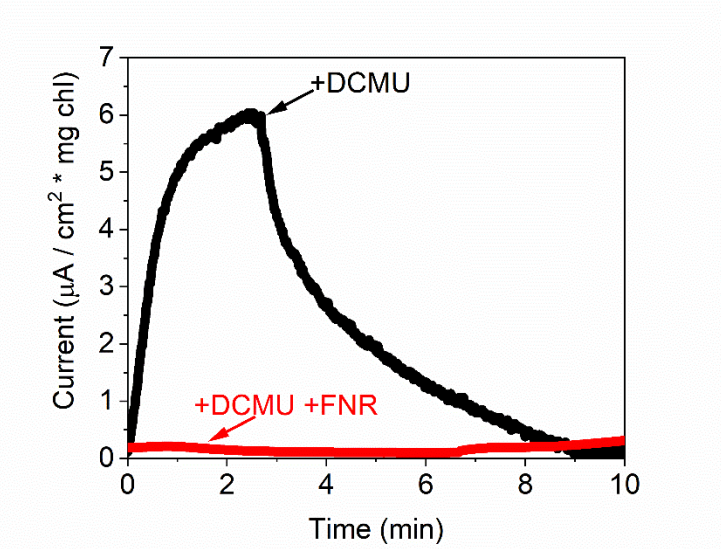

Fig. S8 – FNR abrogates the photocurrent also in the presence of DCMU, Related to Fig. 5. In order to conclude whether addition of DCMU increase the photocurrent by releasing a new electron mediator(s) different from NADPH, CA of *Syn* + 200 µM DCMU with or without 1 mg / mL FNR were measured. Addition of DCMU increased the photocurrent. however, when FNR was also added, it still totally abrogated the photocurrent. This result indicates that NADPH is the major electron mediator also when DCMU is added. CA of *Syn* + DCMU (black), *Syn* + DCMU + FNR (red).

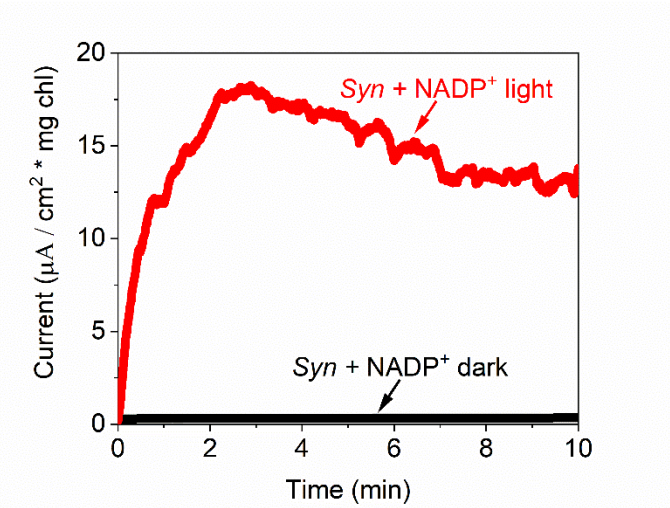

Fig. S9 – Addition of $NADP^+$ to *Syn* did not produce current in dark. Related to Fig. 6. Although *Syn* does not produce current in dark, the possibility that $NADP^+$ can produce current by mediating electrons in the dark was examined. CA of *Syn was* measured in dark and light with addition of 5 mM $NADP^+$ after pre - incubation of 2 h (in 5 mM $NADP^+$). No photocurrent was produced in the dark. CA of *Syn* + 5 mM $NADP^+$ in dark (black), CA of *Syn* + 5 mM $NADP^+$ in light (red).

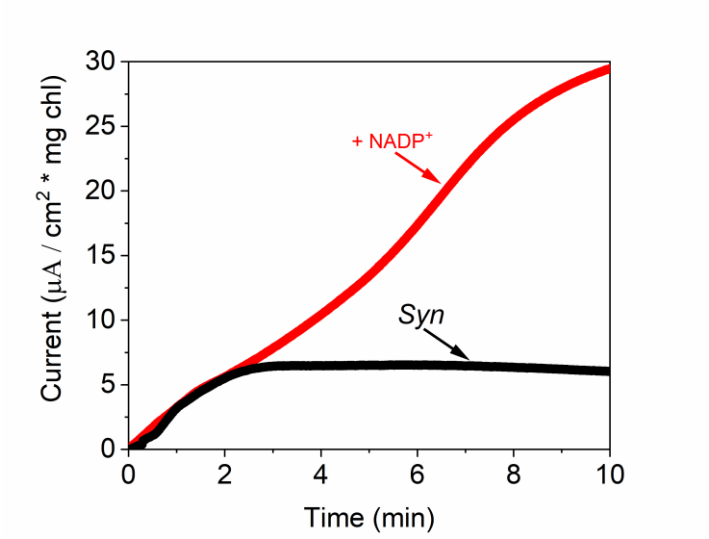

Fig. S10 – Addition of NADP$^+$ increases the photocurrent also in the larger BPEC. Related to Fig. 6. In order to show that NADP$^+$ has the potential to increase the photocurrent in the large BPECs (Saper et al., 2018). CA of *Syn* with or without addition of 5 mM NADP$^+$ was measured in the large BPEC. Addition of NADP$^+$ has increased the photocurrent from ~6 to 30 µA / cm^2 * mg chl. CA of *Syn* (black), CA of *Syn* + 5 mM NADP$^+$ (red).

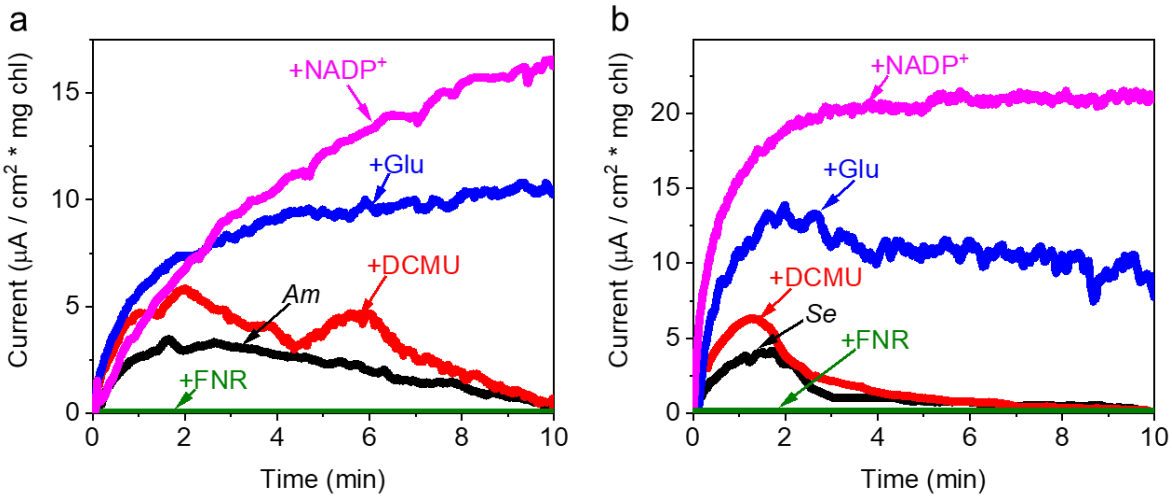

Fig. S11 - *Am* and *Se* also increase their photocurrent production in the presence of exogenous glucose (Glu), DCMU, and NADP$^+$ and do not produce current in the presence of FNR, Related to Fig. 7. CA of *Am* and *Se* without and with DCMU, Glu, NADP$^+$ and FNR were measured. Both species showed a similar pattern to *Syn* in which addition of DCMU, Glu and NADP$^+$ has increased the photocurrent and FNR has almost totally abrogated the current. Based on this finding, we suggest that the same mechanisms for photocurrent production which exist in *Syn* are probably general for many other cyanobacterial species. **a** CA of *Am* (black), *Am* + DCMU (red), *Am* + Glu (blue), *Am* + NADP$^+$ (magenta) and *Am* + FNR (green). **b** CA of *Se* (black), *Se* + DCMU (red), *Se* + Glu (blue), *Se* + NADP$^+$ (magenta) and *Se* + FNR (green). Addition of Glucose and NADP$^+$ were done 1 and 2 h before the beginning of each measurement, respectively, and the incubation was done in the dark. Addition of DCMU and FNR was done right before the beginning of the measurement.

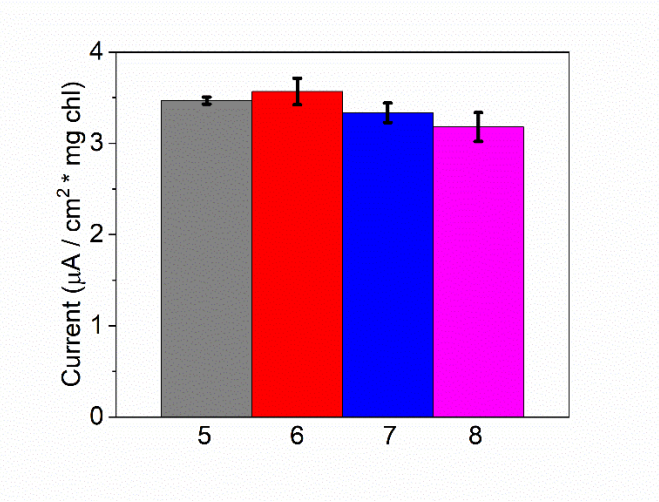

Fig. S12. pH optimization of *Syn* CA in the miniBPEC. Related to the Transparent Methods section. CA of *Syn* was measured in MES buffer with different pH values. The maximal photocurrent was obtained at pH = 6. However, the current was not significantly higher than in pH values of 5, 7 and 8. The bars display the maximal photocurrent of 3 independent measurements at pH values of 5 (grey), 6 (red), 7 (blue) and 8 (magenta).

References

Bar-Zvi, S., Lahav, A., Harris, D., Niedzwiedzki, D.M., Blankenship, R.E., and Adir, N. (2018). Structural heterogeneity leads to functional homogeneity in A. marina phycocyanin. Biochim. Biophys. Acta - Bioenerg. *1859*, 544–553.

Fish, A., Lebendiker, M., Nechushtai, R., and Livnah, O. (2003). Purification, crystallization and preliminary X-ray analysis of ferredoxin isolated from thermophilic cyanobacterium Mastigocladus laminosus. Acta Crystallogr. Sect. D *59*, 734–736.

Lawaetz, A.J., and Stedmon, C.A. (2009). Fluorescence intensity calibration using the Raman scatter peak of water. Appl. Spectrosc. *63*, 936–940.

Marco, P., Elman, T., and Yacoby, I. (2019). Binding of ferredoxin NADP+ oxidoreductase (FNR) to plant photosystem I. Biochim. Biophys. Acta - Bioenerg. *1860*, 689–698.

Ritchie, R.J. (2008). Universal chlorophyll equations for estimating chlorophylls a, b, c, and d and total chlorophylls in natural assemblages of photosynthetic organisms using acetone, methanol, or ethanol solvents. Photosynthetica. *46*, 115–126.

Ritchie, R.J. (2006). Consistent sets of spectrophotometric chlorophyll equations for acetone, methanol and ethanol solvents. Photosynth. Res. *89*, 27–41.

Saper, G., Kallmann, D., Conzuelo, F., Zhao, F., Tóth, T.N., Liveanu, V., Meir, S., Szymanski, J., Aharoni, A., Schuhmann, W., Rothschild, A., Schuster, G., and Adir, N. (2018). Live cyanobacteria produce photocurrent and hydrogen using both the respiratory and photosynthetic systems. Nat. Commun. *9*.